ANTIBODY-DRUG-CONJUGATES AS TARGETED CHEMOTHERAPY AGENTS FOR BREAST CANCER

by

Salli Gür

B.S., Chemistry, Boğaziçi University, 2017

Submitted to the Institute for Graduate Studies in
Science and Engineering in partial fulfillment of
the requirements for the degree of
Master of Science

Graduate Program in Chemistry
Boğaziçi University
2019

To my family

ACKNOWLEDGEMENTS

I would like to express my most sincere gratitude to my thesis supervisor Prof. Rana SANYAL for being a great advisor. Her ideas and tremendous support had a major influence on this thesis. I appreciate her endless patience, attention and encouragement throughout this study. It was great pleasure for me to work with her.

I would extend my thanks to Prof. Amitav SANYAL for his all helpful discussions regarding all my research in this laboratory and for his help during my masters program.

I wish to express my thanks to Assist. Prof. Özgül Gök for her careful and constructive review of the final manuscript and for her care and help during my masters program.

I also thank all my labmates for her generous help during my research besides enjoyful friendship. Especially, I am so much thankful to Burcu Sümer, Merve Karaçivi, Sefa Baki and Enfal Özer for their contribution to my research and their supportive friendships.

I would wish to thank my friends Aysun Değirmenci, Refia Tığrak and Ayşe Zeyneb Erten for their intimate friendships and supports in every part of my life.

My deepest thanks go to my family for their endless support during all of my education.

This research has been supported by The Scientific and Technological Research Council of Turkey (TÜBİTAK) (117Z324). I want to thank to TÜBİTAK.

ABSTRACT

ANTIBODY-DRUG-CONJUGATES AS TARGETED CHEMOTHERAPY AGENTS FOR BREAST CANCER

Antibodies are large molecular weight proteins produced by the immune system. They have high affinity to receptors on different cells' surfaces. Using this affinity, a number of studies have been conducted to deliver cytotoxic drugs to the tumor cell. Antibody-drug conjugates (ADCs) are monoclonal antibodies conjugated with cytotoxic molecules by a suitable linker. They have made a fundamental change in the field of chemotherapy [1]. Many trials on ADCs have been carried out in the clinic. The major feature of ADCs is to enable targeted drug delivery to the desired part of the body. This feature paves the way to increase therapeutic efficacy on target cells while it reduces cytotoxicity on non-targeted cells. In this thesis, a novel ADC based on Trastuzumab (Tmab) and poly (ethylene glycol) was designed. Using a biodegradable linker, drug molecules are conjugated to the polymer which in turn is conjugated to Tmab. The overall aim of increasing the payload on the targeting moiety is realized.

ÖZET

MEME KANSERİ İÇİN HEDEFLİ KEMOTERAPİ AJANI OLARAK ANTİKOR-İLAÇ-KONJUGTLARI

Antikorlar, bağışıklık sistemi tarafından üretilen büyük moleküler ağırlıklı proteinlerdir. Farklı hücrelerin yüzeylerindeki reseptörlere yüksek afiniteleri bulunmaktadır. Bu afinite kullanılarak, sitotoksik ilaçların tümör hücresine iletilmesi için birçok çalışma yapılmıştır. Antikor-ilaç konjugatları (ADC'ler) uygun bir bağlayıcı vasıtasıyla sitotoksik moleküller ile konjuge edilmiş monoklonal antikorlarıdır. Kemoterapi alanında temel bir değişiklik yapmışlarıdr [1]. Klinikte ADC'lerle ilgili birçok çalışma yapılmıştır. ADC'lerin ana özelliği, vücudun istenen kısmına hedeflenen ilaç dağıtımını sağlamaktır. Bu özellik, hedefli olmayan hücrelerde sitotoksisiteyi azaltırken, hedefli hücrelerde terapötik etkinliği arttırmanın yolunu açmaktadır. Bu tezde, Trastuzumab (Tmab) ve poli (etilen glikol) bazlı yeni bir ADC tasarlanmıştır. Biyobozunur bir bağlayıcı kullanarak ilaç molekülleri, sırayla Tmab'a konjuge olan polimere konjuge edilir. Hedef kitledeki yükün arttırılması hedefinin tamamı gerçekleştirilmiştir.

TABLE OF CONTENTS

LIST OF FIGURES

LIST OF TABLES

LIST OF ACRONYMS/ABBREVIATIONS

ACN	Acetonitrile
AIBN	2,2′-Azobis(2-methylpropionitrile)
ATR-FT-IR	Attenuated Total Reflection Fourier Transform Infrared
BCA	Bicinchoninic Acid
CCK-8	Cell Counting Kit-8
$CDCl_3$	Deuterated Chloroform
CDTPA	4-Cyano-4- (dodecyl sulfonyl thiocarbonyl) sulfonyl pentanoic acid
CH_2Cl_2	Dichloromethane
CTA	ChainTransfer Agent
DAR	Drug Antibody ratio
DCC	N,N'-Dicyclohexylcarbodiimide
DCU	Dicyclohexylurea
DIPC	N,N'-Diisopropylcarbodiimide
DLS	Dynamic Light Scattering
DMAc	Dimethylacetamide
DMAP	4-Dimethylaminopyridine
DMF	N,N-Dimethylformamide
DMSO	Dimethyl sulfoxide

DTX	Docetaxel
EDCI	1-Ethyl-3-(3-Dimethylaminopropyl) Carbodiimide
EtOAc	Ethyl acetate
EPR	Enhanced Permeability and Retention
FDA	Food and Drug Administration
FMA	Fluorescein-O-methacrylate
FT-IR	Fourier Transform Infrared
GFLG	Glycine-Phenylalanine-Leucine-Glycine
GPC	Gel Permeation Chromatography
GSH	Glutathione
HER2	Human Epidermal Growth Factor Receptor Type 2
HUVEC	Human Umbilical Vein Endothelial Cell
J	Coupling Constant
kDa	Kilo Dalton
LC-MS	Liquid Chromatography–Mass Spectrometry
LC-MS-MS	Liquid Chromatography–Mass Spectrometry- Mass Spectrometry
MA	Methacrylate
MA-GFLG-DTX	Methacrylic -Gly-Phe-Leu-Gly-Docetaxel
MA-GFLG-OH	Methacrylic -Gly-Phe-Leu-Gly

MALDI-TOF	Matrix-assisted laser desorption/ionization-Time of Flight
MeOH	Methanol
MHz	Mega Hertz
MTD	Maximum Tolerated Dose
NMR	Nuclear Magnetic Resonance
OEGMEMA	Poly(ethylene glycol) methyl methacrylate
PAR	Polymer Antibody Ratio
PBS	Phosphate Buffer Saline
PDI	Polydispersity index
PDS	2- (pyridin-2-yldisulfanyl) ethanol
PDS-CDTPA	2- (pyridin-2-yldisulfanyl) ethyl 4-cyano-4-(((dodecylthio) carbonothioyl) thio) pentanoate
PEG	Poly(ethylene glycol)
RAFT	Reversible Addition- fragmentation Chain Transfer
Rpm	Rounds per minute
rt	Room Temperature
SEC-MALLS	Size Exclusion Chromatography- Multi-Angle Light Scattering
TFA	Trifluoroacetic acid
Tmab	Trastuzumab
UV	Ultraviolet

1. INTRODUCTION

1.1. Cancer

Cancer is the name of a collection of related diseases [2]. In normal cells, cells grow and when they grow old or are damaged, they die. A cell's life normally is such this process. However, this orderly process is invalid for cancer cells. Cancer cells begin to divide without stopping and spread into surrounding tissues in all types of cancer (Figure 1.1) [2]. According to the World Health Organization (WHO), cancer is the second reason for death in the world and 9.6 million people died due to different type of cancer in 2018. The most common cancer types are lung, breast, colorectal, prostate, skin cancer and stomach [3]. In general, surgery, chemotherapy, and radiation therapy are used for cancer treatment. In addition to these, the usage of targeted therapy has been becoming widespread.

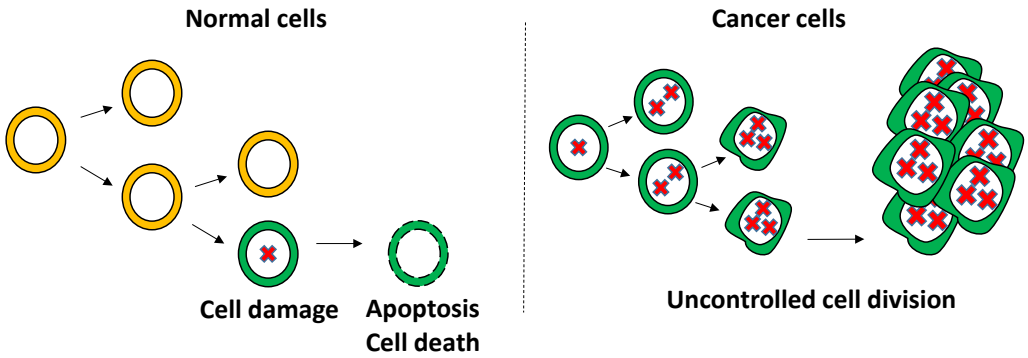

Figure 1.1. Schematic representation of normal and cancer cell growth.

1.2. Targeted Drug Delivery

Targeted drug delivery uses cytotoxic drugs in the cancer treatment to control the biodistribution and bioavailability profile of the drugs in the body. In the mechanism of targeting drug delivery, drug is loaded to vesicles that are any targeting drug delivery systems such as polymeric micelles or polymer-drug conjugates, after consuming of vesicles, vesicles travel to targeted sites such as cancer's specific genes, proteins, or the tissue environment

that contribute to cancer growth and survival [4] and vesicles release cytotoxic drugs to only kill cancer cells in here (Figure 1.2).

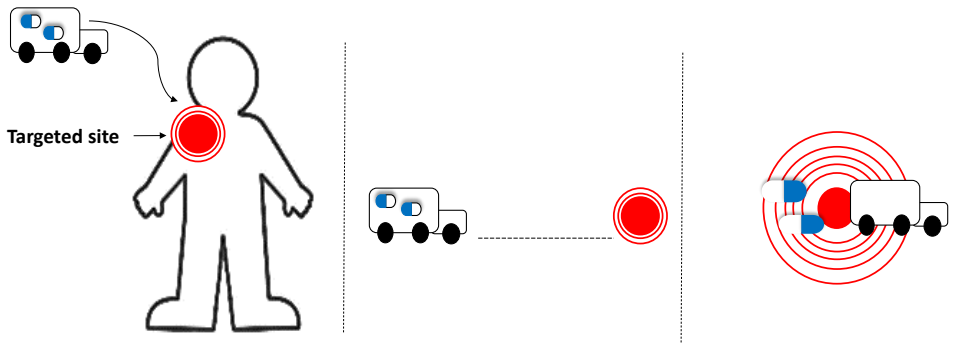

Figure 1. 2. Schematic representation of targeted drug delivery.

However, in chemotherapy, anticancer drugs cannot discriminate healthy and cancerous cells and they can spread to all of body, which causes some problems. One problem is the low therapeutic window of free drugs, which causes dose related toxicity such as gastrointestinal disorders, cardiotoxicity, and extravasation [5]. Another problem is that chemotherapeutic drugs lead to decrease in the amount of bone marrow cells, this is called as myelosuppression. These cells are important for the production of white blood cells that have a function in the defense mechanism of organisms. Due to this, people that use anticancer drugs have a weak immune system. The other common problems are solubility and half-life of drugs. If anticancer drugs are hydrophobic, they are not soluble in the blood, on the other hand, if they are soluble, they have a short half-life and renal clearance in the body [6]. Due to all of these problems, they don't have enough efficiency to cure people.

Therefore, by considering all these limitation, using targeting drug delivery provides reduction of drug side effects, broad therapeutic window and better pharmacokinetic profile. There are two ways to obtain targeted drug delivery via drug loaded nanocarriers (Figure 1.3) passive and active targeting [7].

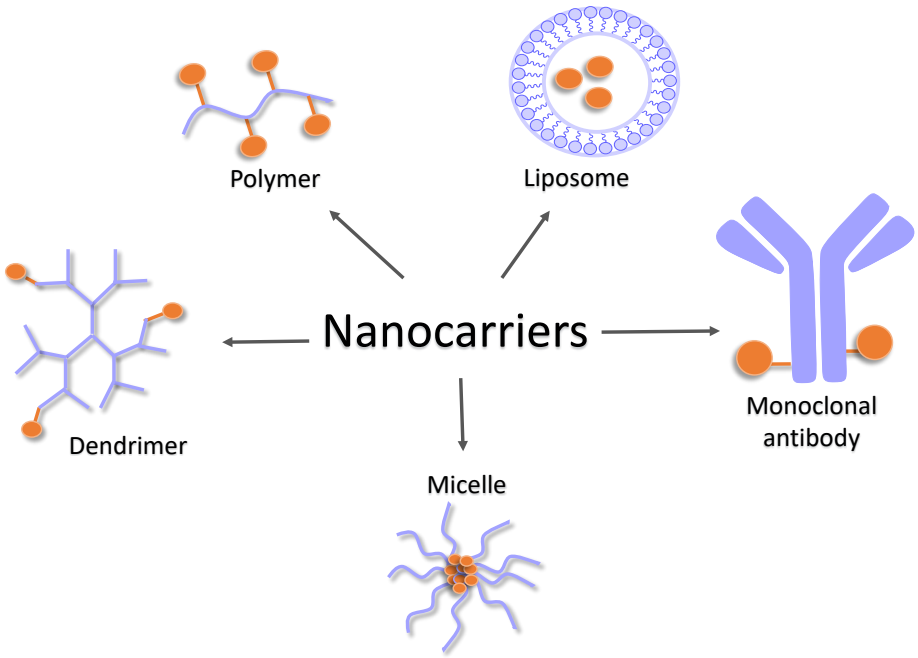

Figure 1.3. General illustration of nanocarrier systems.

1.2.1. Passive Targeting

The EPR effect is a common phenomenon based on hyper permeability of tumor vessels allowing particles or macromolecules to enter tumor space and EPR effect provides particles or macromolecules to stay there for a long time due to lack of lymphatic drainage system. In the tumor blood vessels, endothelial cells consist of large gaps. Because of large gaps, tumor tissues show retention of macromolecular drug above 40 kDa and nanostructures more than 100 nm size. In contrast, size of normal vessel wall is less than 10 nm, so therapeutic particles with size larger than 10nm will not be able to extravasate to normal tissues. As a result, drug delivery systems selectively pass through tumor vessels and they accumulate in there by circulating in blood stream and they show therapeutic effect. In order to target cancer cells through the EPR effect, drug loaded nanocarriers are modified as having enough size to accumulate inside of tumor tissues instead of in normal tissues (Figure 1.4) [8].

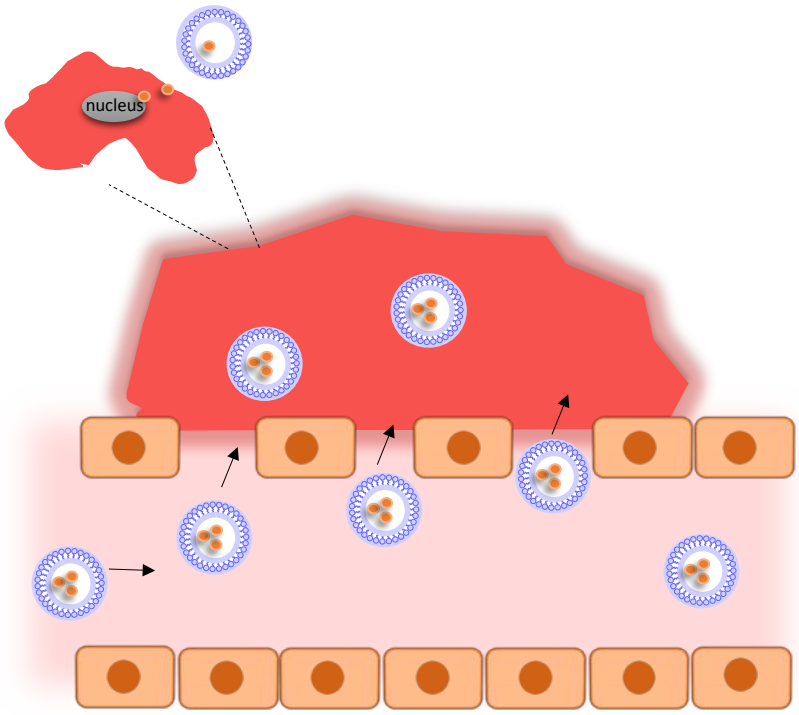

Figure 1.4. Schematic representation of EFR effect.

1.2.2. Active Targeting

There are receptors on the surface of cells, but in cancer cells, these receptors are overexpressed. Drug loaded nanocarriers are designed to make a conjugation between a specific receptor and ligand by using high affinity between them. In this way, targeting ligands carried by nanocarriers bind to receptors on the surface of tumor cells, after specific conjugation, they are internalized by cells and the number of drugs transported to tumor cells is more than healthy cells (Figure 1.5) [9]. Targeted therapy can be collected under two headings that are small molecules and monoclonal antibodies. Gefitinib that targets the epidermal growth factor receptor (EGFR) tyrosine kinase for non-small cell lung cancer [10] and VAL-083 that is a “first-in-class” DNA-targeting agent with a unique bi-functional DNA cross-linking mechanism [11] are examples for small molecules. Trastuzumab that targets the Her2 receptor expressed in some types of breast cancer [12] and Brentuximab targets the cell-membrane protein CD30 are examples for monoclonal antibodies [13].

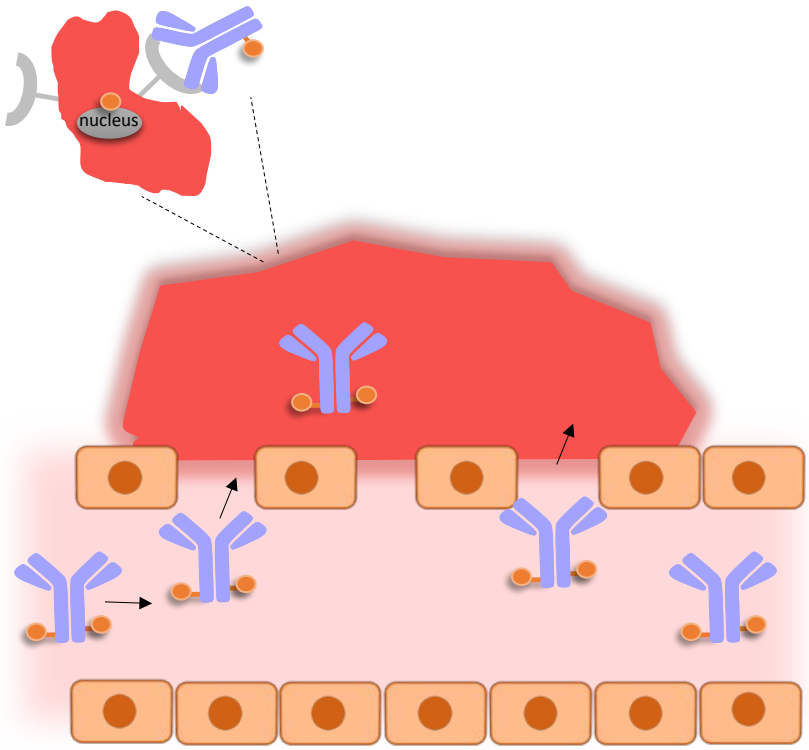

Figure 1.5. Schematic representation of active targeting.

1.3. Antibody-Drug Conjugates (ADCs)

Over the past half century, cancer treatment has improved significantly along with usage and the progress of chemotherapy [14]. To prevent cell division and growth out of control, chemotherapy is one of the most common therapeutic strategies. Other methods are surgery, radiation, targeted and immune therapy. The aim of all methods is to cure cancer and prolong the life of patients. Generally, there are three goals of chemotherapy and these are cure, control and palliation. Cytotoxic drugs used in chemotherapy cause cell death by inhibiting DNA synthesis, microtubule or protein function. However, besides of success of chemotherapy in cancer treatment, there are some severe side effects due to off-targeted cytotoxicity, which may make worse patients' life quality and cause the end of chemotherapy in some cases. Based on these disadvantages of chemotherapy, some scientists focus on creating highly cytotoxic drugs conjugated with cell targeted molecules. Especially, the design of ADC, monoclonal antibodies conjugated with cytotoxic drugs via suitable linkers, has started a new era in the cancer chemotherapy. Selective delivery of cytotoxic drugs

provided by ADCs enhances efficacy, decreases systematic toxicity , and also enables preferable pharmacodynamics (PD) / pharmacokinetics (PK) and biodistribution compared to traditional chemotherapy [1].

1.3.1. History of ADCs

In 1913, German physician and scientist Paul Ehrlich offered the concept of selective delivery of cytotoxic drugs to targeted cell [15]. After 45 years, his targeted therapy idea was shown under the title of ADC and methotrexate was conjugated with leukemia cell targeting antibody [16]. Then, the number of clinical trials related to ADCs has been increased and antibody engineering has been advanced in terms of technology and literature. After significant efforts, FDA-approved ADCs was launched and they are gemtuzumab ozogamicin (Mylotarg®) in 2000 for CD33-positive acute myelogenous leukemia [17], brentuximab vedotin (Adcetris®) in 2011 for CD30-positive Hodgkin's lymphoma and systemic anaplastic large cell lymphoma [18], and trastuzumab emtansine (Kadcyla®) in 2013 for HER2-positive breast cancer [19].

1.3.2. Structure and Mechanism of ADCs

ADCs consist of four components that are monoclonal antibody, cytotoxic agent, conjugation part and linker (Figure 1.6). Monoclonal antibody targets the specific cancer part and provides low cytotoxicity to off-targeted cells, low immunogenicity and maintains binding, stability and internalization to cytotoxic drugs. Cytotoxic agent kills or damages cells. Conjugation and linker part are also crucial for ADCs construction. Linker covalently connects antibody with cytotoxic agents by using chemistry in the conjugation part. Cleavable or non-cleavable linkers are examples for linker parts such as hydrazone, disulfide and enzymatically cleavable linker, and lysine coupling and cysteine alkylation are examples for the conjugation part [1].

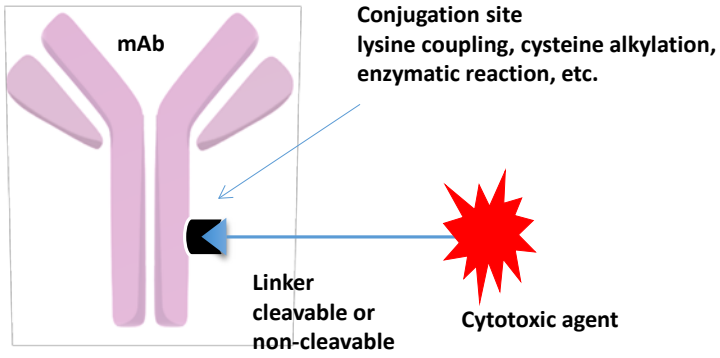

Figure 1.6. The structure and components of antibody drug conjugate.

In recent years, humanized monoclonal antibodies are preferred because they enable high cell target specificity, long circulation time in the blood and minimal immunogenicity. After conjugation with cytotoxic drugs, they provide high potency to targeted cells and reduce cytotoxicity to off-targeted cells. General action mechanism of ADCs starts after administration of ADCs into blood stream. Then, antibody parts of ADCs recognize and bind its specific cell-surface antigen overexpressed in targeted cells. Through endocytosis, ADC-antigen complex is internalized and after lysosomal degradation, cytotoxic drugs are released as a bioactive form inside the cell. These drugs can damage DNA strands or microtubules or exert RNA polymerase inhibition, which causes cell death (Figure 1.7).

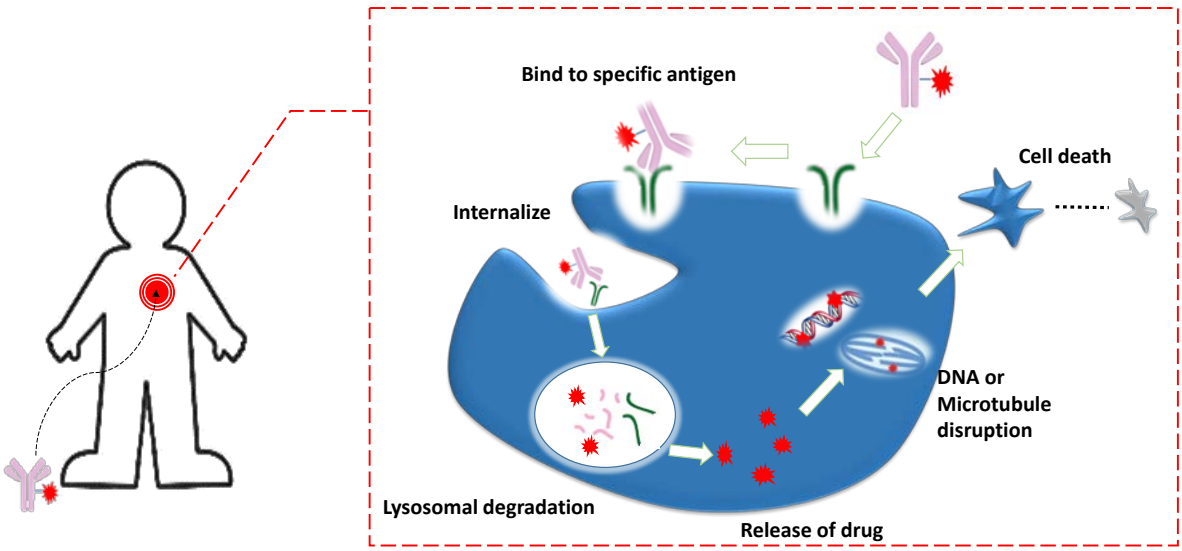

Figure 1.7. Schematic representation of the mechanism of ADC.

1.3.3. Choice of Antigen and Cytotoxic Agent

As seen in the mechanism (Figure 1.7), the first key of the ideal ADC is sufficient affinity and specificity of antibody towards to its antigen. Antibodies with extremely high affinity to their antigens cause reduced efficiency of solid tumor penetration [20]. Moreover, antigens must be overexpressed in the cancer cells than in healthy cells in order to obtain efficient delivery of cytotoxic drugs and selective cancer cell death, which plays an important key role in the determination of therapeutic window. Indeed, there are some studies, and these propose the relation between ADC efficacy and antigen density depend on the type of cancer due to changing the internalization rate of ADC-antigen complex [21].

The other key point is the cytotoxicity and the number of cytotoxic agents on antibody. Some researchers show that if the efficiency of administered ADCs after each step in the mechanism is supposed as 50%, only 1.56% of drugs can get into targeted cells [22]. Therefore, cytotoxic drugs should be highly enough potency to eliminate targeted tumor cells, nearly in the picomolar range, but not to be toxic off-targeted cells in the body. For example, antimitotic drugs such as maytansinoids (used in Kadcyla®) and auristatins (used in Adcetris®) are less toxic to noncancerous cells than cancer cells [19].

1.3.4. Conjugation and Linker Chemistry for ADCs

The linker covalently binds antibody to cytotoxic drugs and its chemical design and properties are important to achieve high ADC efficacy. In the ADC system, some issues should be taken into consideration during choosing of linker. The first issue is stability of linker. The linker should be stable during circulation in plasma and ADC should localize in tumor site and release cytotoxic drugs in here. If the linker isn’t stable, it causes premature release of cytotoxic drugs and it damages healthy cells, which results in systemic toxicity and side effects. Secondly, the linker should be cleavable and release cytotoxic drugs from antibody after ADC is internalized into targeted tumor cells. In addition to these two issues, the hydrophobicity of linker is crucial because hydrophobic drugs coupled with hydrophobic linker often lead to aggregation and rapid clearance. An example for aggregation is that King and co-workers conjugated monoclonal antibody (BR96) with doxorubicin through hydrophobic peptide based linker [23]. Aggregated ADCs tend to rapidly be cleaned by liver,

which causes hepatotoxicity [24]. In addition to this, aggregated ADCs can treat as immunogenic substance and trigger undesired immune response during circulation in the snegatively charged sulfonate groups [26], or pyrophosphate di-ester groups [27]. Zhao and co-workers synthesized linkers that contain negatively charged sulfonate groups and PEG bound to N-hydroxysuccinimide (NHS) ester and by using these linker, they made different conjugations with maytansinoid. Their results showed that when they compared their ADC with previous ADCs that contain hydrophobic SMCC and SPDB linkers, they increased DAR from 3.6 to 6.6 with sulfonate based linker and this enhanced the potency of ADC towards to cancer cell lines in vitro and tumor xenograft models in vivo [26].

1.3.4.1. Chemical Conjugation. Chemical conjugation in ADCs is carried out through amino acid groups on the surface of antibody. After conjugation, the mixture of ADCs is created with variable Drug-Antibody Ratio (DAR). However, the broad distribution of DAR leads to reduced ADC efficacy, so this distribution should be controlled. Otherwise, high DAR can increase potency, aggregation and clearance. Therefore, ideal DAR with controlled distribution can enhance tolerability, efficacy and cytotoxic profile [1]. Lysine amide coupling and cysteine coupling are examples of chemical conjugation chemistry (Figure 1.8).

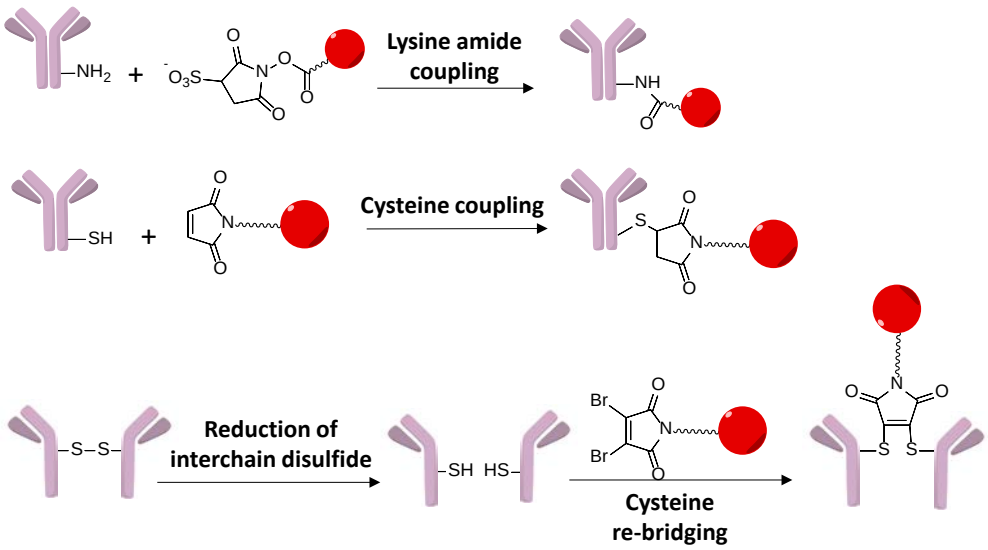

Figure 1.8. Some examples for methods of chemical conjugation.

The lysine amide coupling is one of the most common methods for chemical conjugation because amide coupling between an amine and an activated carboxylic acid is reliable and gives high yield in organic synthesis. Indeed, there are nearly 80 amine residues on the surface of standard antibody, but only 10 of them can give a reaction chemically [28]. However, this conjugation method often results in a broad distribution of ADCs. For example, a maytansinoid type of ADCs has averagely 3.5-4 as DAR and its distribution is between 0-7 [29]. Furthermore, some lysine groups are important for antibody-antigen interaction, so if these lysine groups are used, binding affinity can be decreased.

Cysteine coupling occurs between cysteine residues on the surface of antibody and thiol-reactive groups on the linker or the cytotoxic drugs. Indeed, there are no free thiols in the antibody, they are in disulfide form. In human monoclonal antibodies, there are 12 intrachain and 4 interchain disulfide bonds. These 4 interchain disulfide bonds are not important for structural stability of antibody, therefore, they can be reduced at the mild conditions to obtain 2, 4, 6 and 8 free thiols without breaking 12 intrachain disulfide bonds [1]. In this context, using cysteine coupling for conjugation is superior to lysine coupling in order to control DAR and heterogeneity of ADCs. One example to obtain free thiol is that Junutula and co-workers designed an antibody that has only two cysteine residues on it. This method is called as THIOMAB. In this way, high homogeneous ADCs (>90% homogeneity) with controlled DAR as 2 and high efficacy and therapeutic window in vivo are obtained [30]. Another method to control heterogeneity is using cysteine re-bridging. For example, firstly, interchain disulfides are reduced at mild condition and re-bridging is obtained between free thiols on antibody and dibromomaleimide on linker or cytotoxic drugs [31,32].

1.3.4.2. Cleavable Linkers. Cleavable linkers attract more attention than noncleavable ones in the area of ADCs and they are designed as cleavable in different intercellular conditions such as pH and redox potential or cleaved by specific lysosomal enzymes. Also, linkers are designed to release cytotoxic drugs after bond cleavage. Hydrazone linker, Cathepsin B linker, disulfide linker and pyrophosphate linker are examples for cleavable linkers (Figure 1.9).

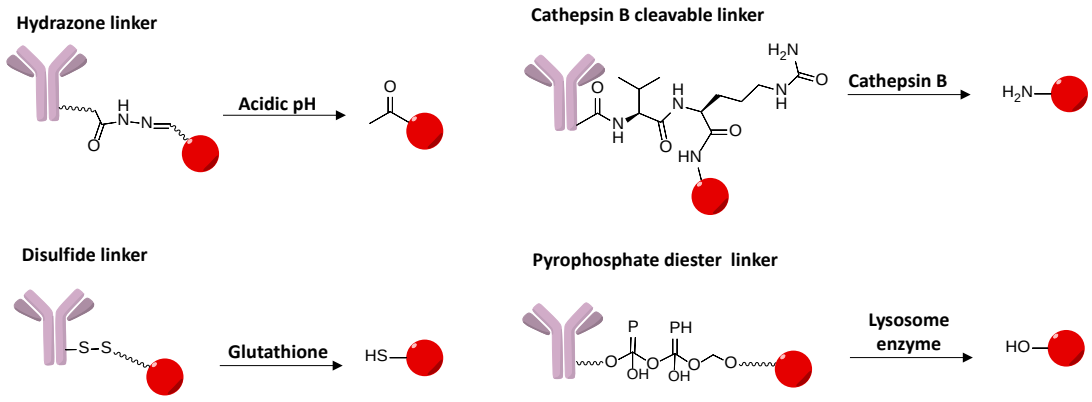

Figure 1.9. General methods for cleavable linkers.

In an acidic medium such as endosome (pH 5-6) and lysosome (pH nearly 4.8), hydrazone linkers are cleaved. For example, BR96 was conjugated with doxorubicin via a hydrazone linker and this ADC was used for metastatic breast cancer [33]. Also, hydrazone linker undergoes slow hydrolysis, so slow release of cytotoxic drugs under physiological conditions (pH 7.4) [34].

Cathepsin B is a lysosomal protease enzyme overexpressed by some cancer cells [35]. Cathepsin B detects certain sequences such as phenylalanine-lysine (Phe-Lys) and valine-citrulline (Val-Cit). Val-Cit coupled with p-aminobenzyloxycarbonyl (Val-Cit-PABC) is a crutial linker for ADCs [36, 37]. After the internalization and endocytosis, in lysosome cathepsin B selectively cleaves the linker (Val-Cit) and this provides the release of cytotoxic drugs from ADCs. For example, Val-Cit-PABC linker is created for brentuximab vedotin (Adcetris®). The PABC part is a spacer between Val-Cit and drug and helps cathepsin B to show its protease activity. Then, the Val-Cit linker is cleaved by cathepsin B to release vedotin [18].

Disulfide linkers are cleaved by glutathione that is overexpressed in the cancer cell cytoplasm (1-10 mmol/L) [38] compared to blood (nearly 5 µmol/L) [39]. In this way, these linkers are stable during circulation, but after internalization, drugs are released by the glutathione existing in the cytoplasm of cancer cells. In addition to this, stability of disulfide linker in blood circulation can be improved further by introducing methyl groups to the

structure. Role of these methyl groups is to increase steric hindrance and slow down the cleavage rate in the presence of low free thiol concentrations.

Pyrophosphate diester linker was developed by Garbaccio and co-workers. This linker has an anionic group, so it has higher water solubility than the other linkers and it has excellent stability during circulation [27]. Pyrophosphate diester linker provides two-step enzymatic cleavage. Monophosphate part firstly is cleaved, then cytotoxic drugs are released. For example, human CD70 antibody was conjugated with glucocorticoids via this linker. Results showed that this ADC has great stability in plasma (nearly 7 days, in vitro) [27].

1.3.4.3. Non-cleavable Linkers. Non-cleavable linkers have stable bonds and show greater stability than cleavable linkers. The release of cytotoxic drugs relies on the degradation of antibody in the cytosolic and lysosome processes. A successful example of this linker is trastuzumab emtansine (Kadcyla) [19], [40].

1.4. Antibody Drug Conjugate for Breast Cancer

According to WHO, breast cancer is the most common cancer and it is the 5th in the cancer deaths [3]. Patients use surgery, chemotherapy, radiation therapy and targeted therapies of the treatment of breast cancer cells. A common example for targeted therapy is trastuzumab (Herceptin®) and it was approved by FDA in 1998 [41]. Trastuzumab targets to HER2 receptor that is a protein made by HER2 gene. Normally, HER2 receptor controls a breast cell's dividing, growing and repeating itself by sending signals to cells. However, if HER2 gene works extraordinary, it causes to increase in the number of HER2 receptor on the surface of breast cells, which results in HER2 positive breast cancer. Therefore, trastuzumab is used for HER2 positive breast cancer because it goes to breast, finds HER2 receptor, bind to it and block the signals that cause cells to grow. However, after advances in the ADC platform, Genentech designed Trastuzumab-DM1 (trade name: Kadcyla®) (Figure 1.10). Trastuzumab-DM1 was designed as delivering emtansine to targeted breast cells by attaching DM1 to trastuzumab. Kadcyla® contains trastuzumab as targeting HER2 receptor, SMCC (Succinimidyl-4-(N-maleimidomethyl) cyclohexane-1-carboxylate) as non-reducible linker and DM1 as killing cancer cells and its DAR is averagely 3.5 [19].

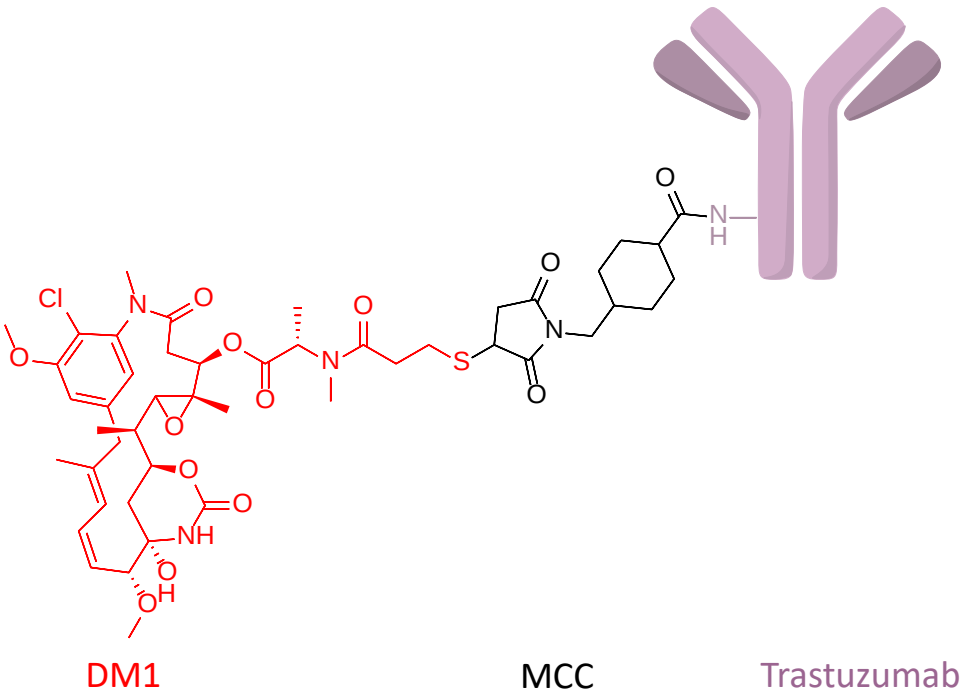

Figure 1.10. The structure of Trastuzumab-DM1.

1.5. Reversible Addition-Fragmentation Chain-Transfer Reaction (RAFT)

RAFT is a polymerization technique and it is discovered by CSIRO in 1998 [42]. The main advantage of RAFT is to control the molecular weights and polydispersities and architectures of polymers. In addition to this advantage, unlike the other controlled radical polymerization types, RAFT provides a wide range of monomers and solvents to synthesize polymers. A radical source, RAFT agent, monomer and solvent are typically required. RAFT agent is crucial for RAFT polymerization because it controls and regulates the polymerization process via R and Z groups on it (Figure 1.11). It can reinitiate the polymerization via R group and it can arrange the activation of C=S bond via Z group [42].

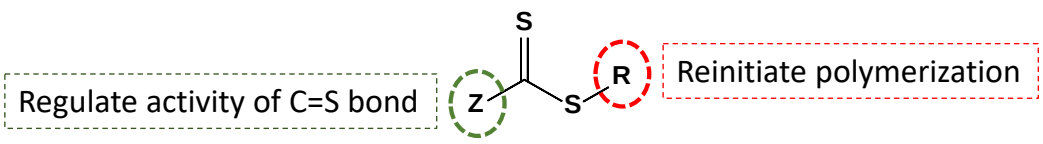

Figure 1.11. General structure of RAFT agent.

In addition to these, RAFT polymerization provides to determine the end groups of polymers [43]. In the literature, people use this end group to remove or change it to be functional in order to use for the next step [44, 45].

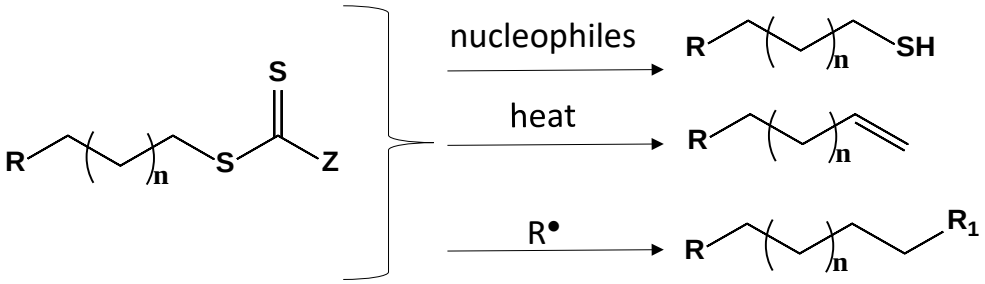

Figure 1.12. Some end group modification reactions from RAFT agent.

2. AIM OF STUDY

Aim of this study is to design and synthesize antibody-polymer drug conjugates (APDC) for treatment of breast cancer. The main purpose of using polymer instead of an antibody-drug conjugate (ADC) system is to increase the drug to antibody ratio (DAR) since each polymer can carry more drugs. In the polymer part of the ADC system, PEG based system is used to increase the aqueous solubility of hydrophobic drug docetaxel (DTX), the circulation time, serum stability and finally the size of ADC system to take advantage of EPR effect. DTX, which inhibits microtubule structures within the cells causing cell death, is chosen as a chemotherapy agent. Furthermore, to attach the drug moiety to the polymer backbone, GLFG linker is selected in order to enable selective drug release. GFLG linker is stable in blood circulation and cleaved by Cathepsin B which is an overexpressed enzyme in the cancer cells. Therefore, DTX is conjugated with cleavable GFLG linker for synthesis of ADC system. FMA (fluorescein methacrylate), which is a fluorescent dye containing monomer, is used to enable characterization of the conjugates. To obtain dye and drug containing polymer, MA-GFLG-DTX, FMA and PEGMA monomers are polymerized by using RAFT polymerization. After synthesizing polymer part of the ADC system, antibody is conjugated to polymer via a cleavable disulfide bond. Trastuzumab, an antibody targeting overexpressed HER2 receptors on the surface of breast cancer, is used for the study. HER2 receptor is overexpressed on breast cancer cells approximately 100 times more than normal breast cells and after binding, trastuzumab also blocks the signals that control cell division and growth. After conjugating trastuzumab and polymer containing PEG, FMA and DTX, the conjugates are purified and characterized.

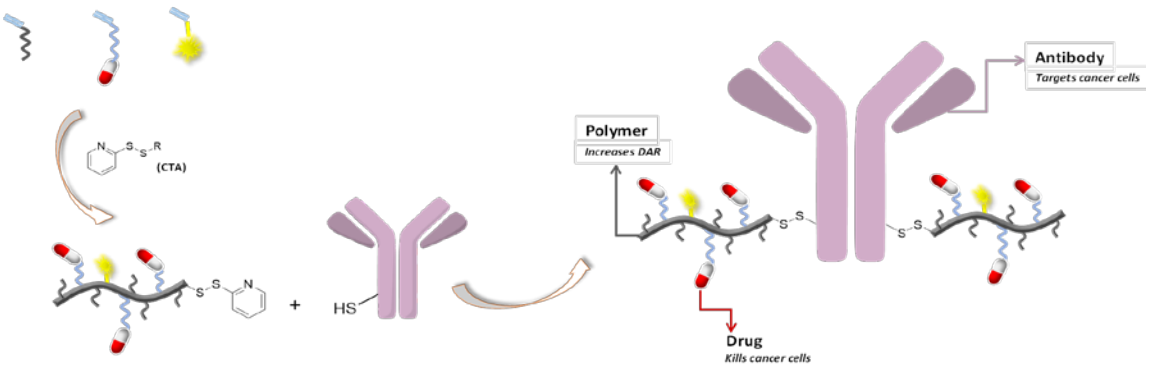

Figure 2.1. Schematic illustration of the aim of the study

3. EXPERIMENTAL

3.1. Materials

Methacryloyl chloride was purchased by Alfa Aesar. 2-mercaptoethanol was purchased by Aldrich. N,N-dicyclohexylcarbodiimide (DCC), 4-Dimethylaminopyridine (DMAP), Fluorescein O-methacrylate (FMA), 2-Iminothiolane and Hydroxybenzotriazole were purchased by Sigma-Aldrich. Herceptin was purchased by Roche. N,N'-Diisopropylcarbodiimide (DIPC) and Aldrithiol was purchased by TCI. LGOH and GFOH were purchased by Bachem. Solvents were obtained from Merck Co. (Germany) and used as received. Anhydrous dichloromethane (DCM) was obtained from SciMatCo purification system. Milli-Q Water Purification System (Milli-Q system, Millipore, Billerica, MA, USA) was used to produce ultrapure water. All the other chemicals were purchased by Sigma-Aldrich. Oligo- (ethylene glycol) methyl ether methacrylate (OEGMA, Mn = 300 g/mol^{-1}) was filtered with basic alumina column, then it was used. 2,2′-Azobis(2- methylpropionitrile) (AIBN) purchased by Sigma-Aldrich was recrystallized from methanol. MA-GF-LG-OH was synthesized according to previously reported protocol [46]. MA-GFLG-DTX monomer was synthesized according to previously reported protocol [47]. 4-cyano-4- (dodecyl sulfanyl thiocarbonyl) sulfanyl pentanoic acid was synthesized according to the procedure [48].

3.2. Instrumentation

^{1}H and ^{13}C NMR spectroscopy (Varian 400 MHz NMR spectrometer), UV−vis spectroscopy (Perkin Elmer series), Fourier transform infrared (ATR-FTIR) spectroscopy (Nicolet 380, Thermo Scientific, USA) instruments were used to characterize synthesized monomers and polymers. The molecular weights were measured by Gel Permeation Chromatography (GPC, Shimadzu, Japan) with a mobile phase solution of 0.05 M lithium bromide in dimethylaceteamide (DMAc) as eluent at a flow rate of 1 mL/min at 30 º C. GPC measurements of polymers were carried out with PSS Win GPC Unity software. PSS Gram (10 μm - 300 × 8 mm) column was calibrated with poly-methyl methacrylate standards, using refractive index detector (RID-10A). During the internalization experiments, cells were

visualized by using Zeiss Observer.Z1 inverted fluorescence microscope. Dynamic Light Scattering (DLS) measurements were done in water and PBS buffer solution at 25 ^{o}C on a Malvern Zetasizer Nano ZS photometer. Akta Avant was used for purification.

3.3. Synthesis of 2-(pyridine-2-yldisulfanyl) ethanol

2,2'-Pyridine disulfide (2 g, 9.08 mol) was dissolved in methanol (6 mL) in a round-bottom flask and this mixture was purged with N_2 gas for 10 min. Firstly, acetic acid (0.13 mL, 2.27 mol) was added to the reaction mixture. Then, 2-mercaptoethanol (0.32 mL, 4.54 mol) that was dissolved in methanol (2 mL) was added to the reaction mixture dropwise. The reaction mixture was stirred for 3 h at 25 °C. After the reaction was completed, MeOH was evaporated under *vacuo* and the reaction mixture was treated with dichloromethane (CH_2Cl_2) (5 mL) and the organic layer was washed with distilled water (30 mL) followed by drying over Na_2SO_4 and evaporation of the solvent. The product was purified by using silica column chromatography. Yellow, viscous product was obtained with 93% yield. ^{1}H NMR ($CDCl_3$, δ, ppm) 8.52 (d, 1 H, *J* = 4.4 Hz), 7.58 (t, 1H, *J* = 8.5 Hz), 7.40 (d, 1H, *J* = 8.0 Hz), 7.16 (t, 1H, *J* = 6.7 Hz), 3.81 (bs, 2H), 2.96 (t, 2H, *J* = 5.0 Hz).

3.4. Synthesis of 2-(pyridin-2-yldisulfanyl) ethyl 4-cyano-4- ((((dodecylthio)) carbonothioyl) thio pentanoate (PDS-CDTPA)

2-(pyridin-2-ylisulfonyl) ethanol (41.7 mg, 0.223 mmol), 4-cyano-4- (dodecyl sulfanyl thiocarbonyl) sulfanyl pentanoic acid (60 mg, 0.148 mmol) and 4-dimethylaminopyridine (DMAP) (18 mg, 0.147 mmol) were dissolved in CH_2Cl_2 (2 mL). The reaction mixture was cooled into 0 ºC by using ice bath and N,N-dicyclohexylcarbodiimide (DCC) (36.8 mg, 0.178 mmol) dissolved in CH_2Cl_2 (2 mL) was added dropwise to the reaction solution. The reaction was stirred at 25 ºC with magnetic stirrer in the dark for 2 days. The resulting dicyclohexylurea (DCU) was filtered. The resulting yellow liquid product was precipitated in MeOH (1 mL). The precipitated solid yellow product was purified by silica column chromatography. (Mobile phase: EtOAc / Hexane (20/80, v / v)). Yellow, viscous product (47 mg, 54 % yield) was obtained. ^{1}H NMR ($CDCl_3$, δ, ppm) 8.49 (d, 1H, *J* = 3.8 Hz), 7.67 - 7.64 (m, 2H), 7.12 (bs, 1H), 4.38 (t, 2H, *J*

= 6.3 Hz), 3.33 (t, 2H, *J* = 7.4 Hz), 3.05 (t, 2H, *J* = 6.3 Hz), 2.63 – 2.33 (m, 4H), 1.87 (s, 3H), 1.68 (dd, 2H, *J* = 14.5, 7.1), 1.39 - 1.26 (m, 18H), 0.88 (t, 3H, *J* = 6.4 Hz).

3.5. Synthesis of PDS-POEGMEMA copolymer

OEGMEMA (100 mg, 0.33 mmol) was dissolved in dioxane (0.5 mL). PDS-CDTPA (5.5 mg, $9.6x10^{-3}$ mmol) dissolved in dioxane (0.25 mL) and AIBN (0.31 mg, 0.18 mmol) dissolved in dioxane (0.25 mL) were added to the reaction. The reaction was stirred in an oil bath at 70 ºC with magnetic stirrer for 19 h. After the reaction, the dioxane was evaporated under *vacuo*. The remaining liquid product was precipitated in diethyl ether for 24 hours in a refrigerator. The mass of the precipitated polymer was determined as 9 kDa by GPC. ^{1}H NMR ($CDCl_3$, δ, ppm) 8.47 (s, 1H), 7.67 (bs, 2H), 7.11 (bs, 1H), 4.2 - 4.0 (m, 20 H), 3.36 (bs, 3H), 0.86 – 2.2 (m, −CH2 and CH3 along with backbone).

3.6. Synthesis of PDS-POEGMEMA-DTX copolymer

OEGMEMA (100 mg, 0.33 mmol) was dissolved in DMF (0.3 mL). PDS-CDTPA (6.8 mg, 0.01 mmol) dissolved in DMF (0.1 mL) and AIBN (0.39 mg, $2.4x10^{-3}$ mmol) dissolved in DMF (0.1 mL) were added to the reaction. MA-GFLG-DTX (45 mg, 0.04 mmol) in DMF (0.4 mL) was added to the reaction mixture. The reaction was stirred in an oil bath at 80 ºC with magnetic stirrer for 72 h. After the reaction, the DMF was evaporated under *vacuo*. The remaining liquid product was precipitated in diethyl ether for 24 h. The product was purified by using dialysis membrane (3.5 kDa) to remove excess monomers which precipitated with the polymer. The mass of the polymer was determined as 10 kDa by GPC. The amount of bulk drug in each polymer chain was calculated as 10.6 % from ^{1}H NMR spectroscopy. ^{1}H NMR ($CDCl_3$, δ, ppm) 8.13 (d, 2H, *J* = 6.9 Hz), 4.2 - 4.0 (m, 20 H), 3.36 (bs, 3H), 0.86 – 2.2 (m, −CH2 and CH3 along with backbone).

3.7. Synthesis of PDS-POEGMEMA-FMA copolymer

OEGMEMA (100 mg, 0.33 mmol) dissolved in DMF (0.3 mL), FMA (0.24 mg, 4x10-4 mmol) dissolved in DMF (0.48 mL), PDS-CDTPA (6.8 mg, 0.01 mmol) dissolved in DMF (0.1 mL) and AIBN (0.39 mg, $2.4x10^{-3}$ mmol) dissolved in DMF (0.1 mL) were

added to the reaction. The reaction was stirred in a 70 ºC and oil bath with a magnetic stirrer. After the reaction, the DMF was evaporated under *vacuo*. The remaining liquid product was precipitated in diethyl ether for 24 h in a refrigerator. The mass of the precipitated polymer was determined as 14 kDa by GPC. The mass in the polymer chain was calculated from ^{1}H NMR spectroscopy as 12 % by mass and as 4 by a number of dyes per polymer. ^{1}H NMR ($CDCl_3$, δ, ppm) 8.42 (bs, 1H), 8.02 (bs, 1H), 3.37 (bs, 3H), 0.86 – 2.2 (m, −CH2 and CH3 along with backbone).

3.8. Synthesis of PDS-POEGMEMA-DTX-FMA copolymer

OEGMEMA (100 mg, 0.33 mmol) dissolved in DMF (0.2 mL), FMA (0.24 mg, 4x10-4 mmol) dissolved in DMF (0.3 mL), PDS-CDTPA (6.8 mg, 0.01 mmol) dissolved in DMF (0.1 mL) and AIBN (0.39 mg, $2.4x10^{-3}$ mmol) dissolved in DMF (0.1 mL) were added to the reaction mixture. MA-GFLG-DTX (45 mg, 0.04 mmol) in DMF (0.3 mL) was added to the reaction mixture. The reaction was stirred in an oil bath at 80 ºC with magnetic stirrer. After the reaction, the DMF was evaporated under *vacuo*. The remaining liquid product was precipitated in diethyl ether for 24 h in a refrigerator. Purification was carried out by using the dialysis membrane (3.5 kDa) to remove excess monomers which precipitated with the polymer. The mass of the polymer was determined as 10 kDa with GPC. The amount of bulk drug in each polymer chain was calculated as 20 % from ^{1}H NMR spectroscopy. ^{1}H NMR ($CDCl_3$, δ, ppm) 8.09 (d, 2H, J = 7.5 Hz), 7.98 (d, 1H, J = 6.1 Hz), 3.33 (bs, 3H), 0.86 – 2.2 (m, −CH2 and CH3 along with backbone).

3.9. Synthesis of Tmab-thiol

2-Iminothiolane (0.27 mg, 0.0019 mmol) was dissolved in PBS (8 mL) buffer solution and trastuzumab (Tmab) (8.1 mg, $5.5x10^{-5}$ mmol) was added to the reaction. The reaction was stirred at 25 ºC for 2.5 hours. The number of thiol functional group bound to Tmab was calculated by the Ellman procedure [49]. According to the result of this procedure, 6 thiols bound to each Tmab. Dialysis was performed with PBS buffer solution and 100 kDa centrifugal filter to remove excess 2-iminothiolane. BCA analysis was performed to find the Tmab concentration and the concentration was obtained as 3.7 mg /mL [50].

3.10. Conjugation of Tmab-PDS-POEGMEMA

Six thiol-containing Tmab-thiol (0.65 mg / mL) and PDS-POEGMEMA (0.5 mg) were dissolved in DMAc (0.05 mL) and PBS (1 mL) buffer solution. The reaction was stirred at room temperature for 18 h. After the reaction was finished, purification was carried out with 100 kDa ultracentrifuge tube.

3.11. Conjugation of Tmab-PDS-POEGMEMA-FMA

Six thiol-containing Tmab-thiol (0.05 mg / mL) and PDS-POEGMEMA-FMA copolymer (0.35 mg) were dissolved in PBS (0.125 mL) buffer solution. The reaction was stirred at room temperature for 18 h. The yellow product was obtained. Purification was carried out firstly with 100 kDa centrifugal filter and then with hydrophobic interaction column chromatography. After using a calibration curve drawn with different concentration of FMA by fluorescence spectroscopy, the PAR ratio was calculated as 2.

4. RESULTS AND DISCUSSION

4.1. Synthesis of 2-(pyridin-2-yldisulfanyl) ethanol

2-(pyridine-2-yl-diulfanyl) ethanol was synthesized by using 2,2-dipyridiyl disulfide and 2-mercaptoethaol in presence of acetic acid in 93 % yield and a new disulfide bond was formed (Figure 4.1).

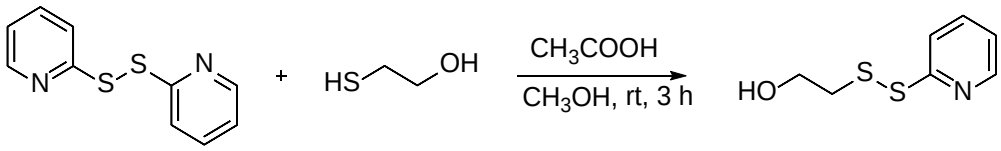

Figure 4.1. The synthesis of 2-(pyridin-2-yldisulfanyl) ethanol.

The product was purified by silica column chromatography, characterized by ^{1} H NMR spectroscopy (Figure 4.2). When ^{1}H NMR spectrum was investigated, aromatic proton signals belonging to pyridine ring were observed between 8.5 - 7.12 ppm. In addition, methylenic protons appeared at 3.81 and 2.96 ppm.

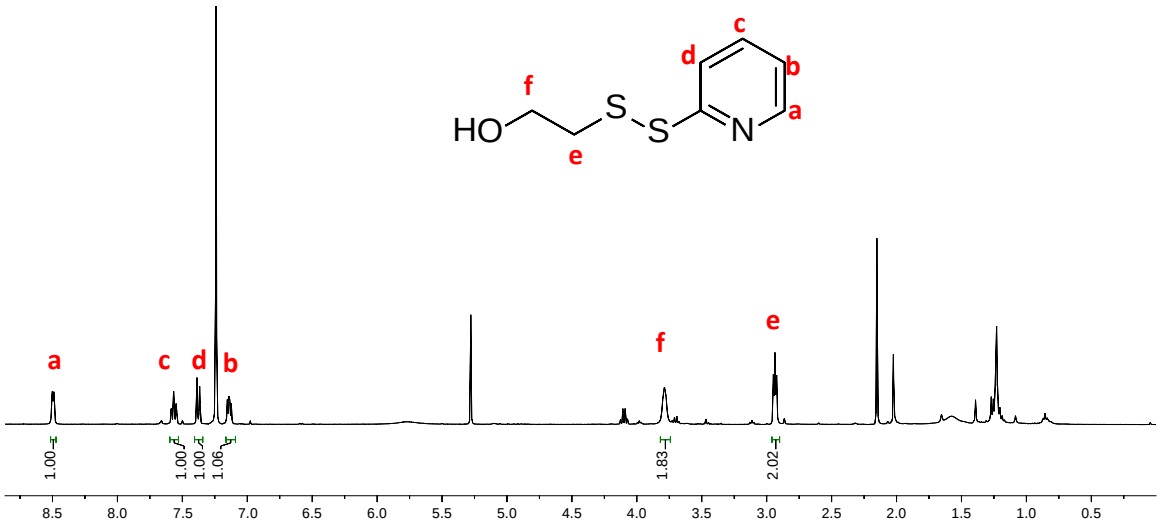

Figure 4.2. ^{1}H NMR spectrum of 2-(pyridin-2-yldisulfanyl) ethanol molecule.

4.2. Synthesis of PDS-CDTPA

PDS-CDTPA was synthesized by using 2-(pyridin-2yldisulfanyl) ethanol and CDTPA via Steglich Esterification in the presence of DCC and DMAP (Figure 4.3). PDS-CDTPA was obtained in 54 % yield.

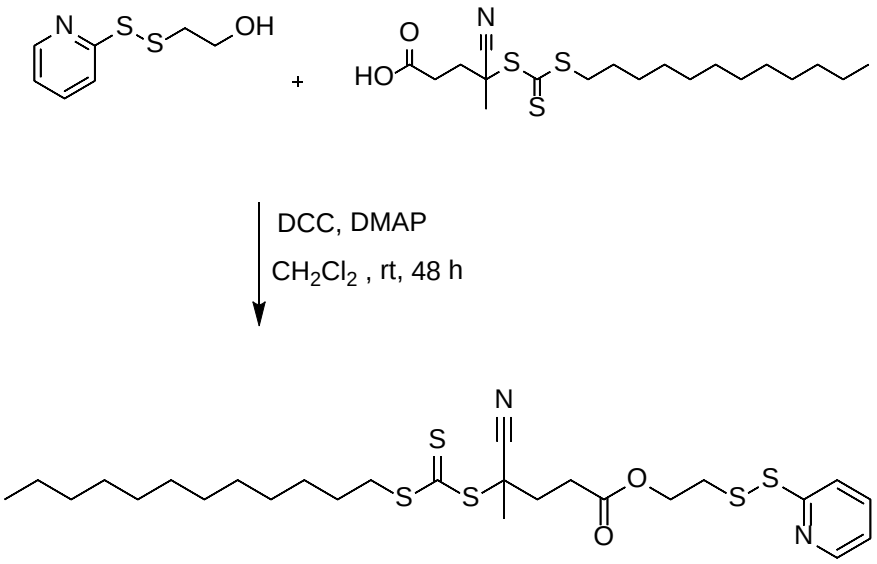

Figure 4.3. The synthesis of PDS-CDTPA molecule.

In order to determine the duration of the reaction, two reactions were carried out by preparing the same amounts of the substance for 24 and 48 hours to be stirred. 38 % yield was obtained for 24 hours, and 54 % yield was obtained for 48 hours. Therefore, the duration of the reaction was chosen as 48 hours. The resulting yellow product was purified by silica column chromatography and characterized by ^{1}H NMR spectroscopy (Figure 4.4). When ^{1}H NMR spectrum was investigated, aromatic proton signals belonging to pyridine ring were observed between 8.5 - 7.12 ppm. In addition, the symbol of h represented methyl group comes from CDTPA and appeared at 1.87. The symbol of d represented –CH_2 group comes from PDS and this peak shifted to 4.38 ppm from 3.81 ppm after esterification reaction.

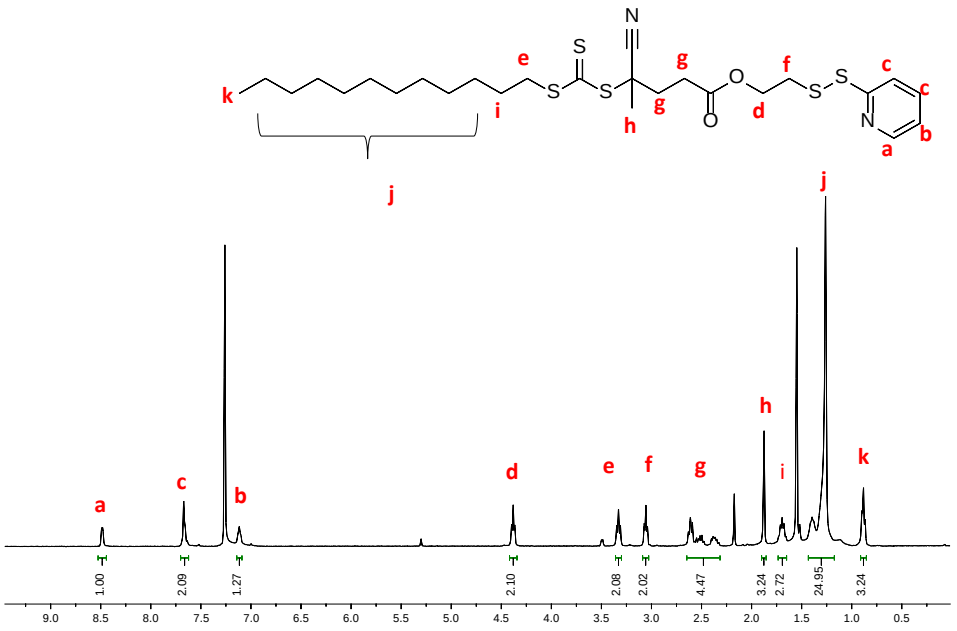

Figure 4.4. ^{1}H NMR spectrum of PDS-CDTPA molecule.

4.3. Synthesis of PDS-POEGMEMA Polymer

The PDS-POEGMEMA was synthesized by using OEGMEMA monomer, AIBN and PDS-CDTPA via Reversible Addition- fragmentation Chain Transfer (RAFT) polymerization technique. AIBN is the radical initiator and PDS-CDTPA is CTA agent and also is used to control the molecular weight of polymer. The equivalents of the reagents and the amount of solvent were changed to establish two different reaction conditions. (Table 4.1).

Table 4.1. Reaction conditions tested for PDS-POEGMEMA polymer synthesis.

	Equivalent			**Dioxane (mL)**	**GPC M_n (kDa)**	**NMR M_n (kDa)**	**M_w/M_n**
	OEGMEMA	**PDS-CDTPA**	**AIBN**				
P1	150	5	1	0.45	No reaction	No reaction	-
P2	175	5	1	1	9	15	1.3

The conditions of the P2 reaction gave the desired molecular weight (Figure 4.5). Molecular weight (Mn) and polydispersity index were measured by using GPC (gel permeation chromatography).

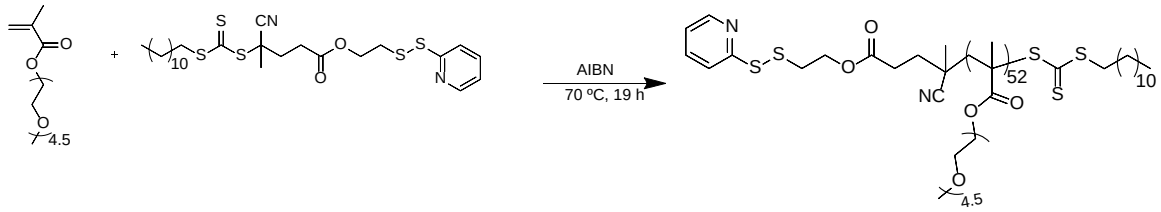

Figure 4.5. The synthesis of PDS-POEGMEMA polymer.

The molecular weight of resulting polymer was determined as 9 kDa by GPC. The ^{1}H NMR characterization of the resulting polymer was performed (Figure 4.6). The signal of pyridine at 8.47 ppm in the PDS-CDTPA molecule confirmed that the PDS-CDTPA molecule was running the polymerization reaction and it was present at the end of the product. The molecular weight of the polymer was calculated as 15 kDa according to ^{1}H NMR spectroscopy.

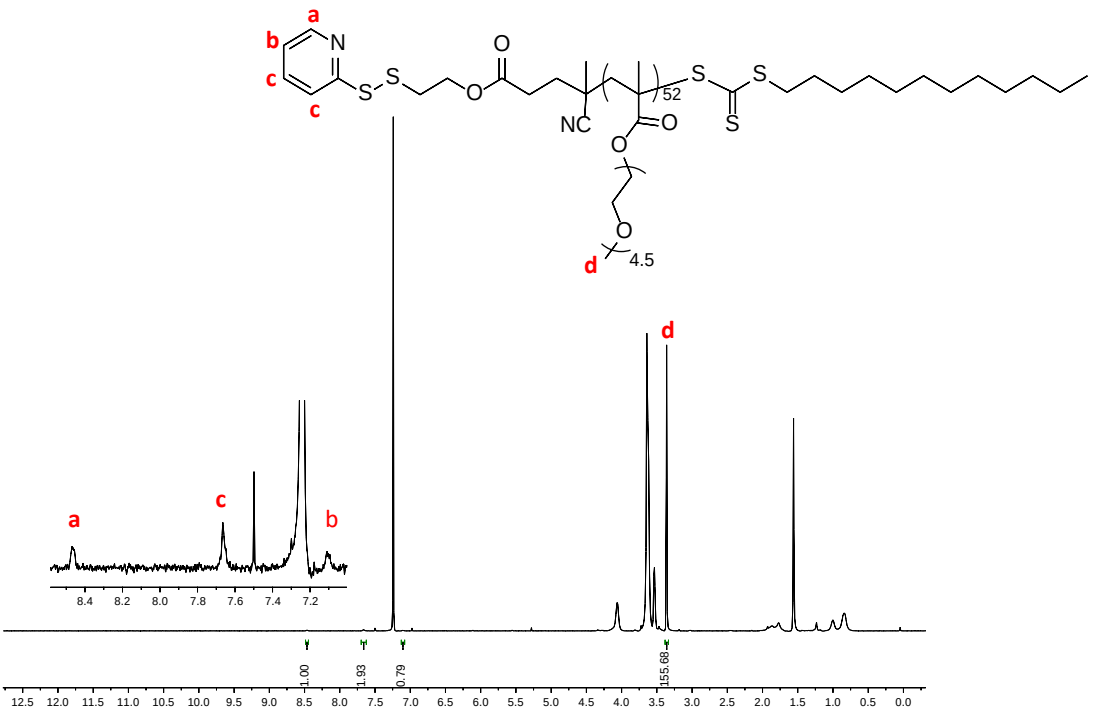

Figure 4.6. ^{1}H NMR spectrum of PDS-POEGMEMA polymer.

4.4. Synthesis of PDS-POEGMEMA-FMA Copolymer

The PDS-POEGMEMA-FMA copolymer was synthesized by using OEGMEMA monomer, Fluorescein O-methacrylate (FMA), AIBN and PDS-CDTPA as a dye-containing polymer via RAFT polymerization technique (Figure 4.7).

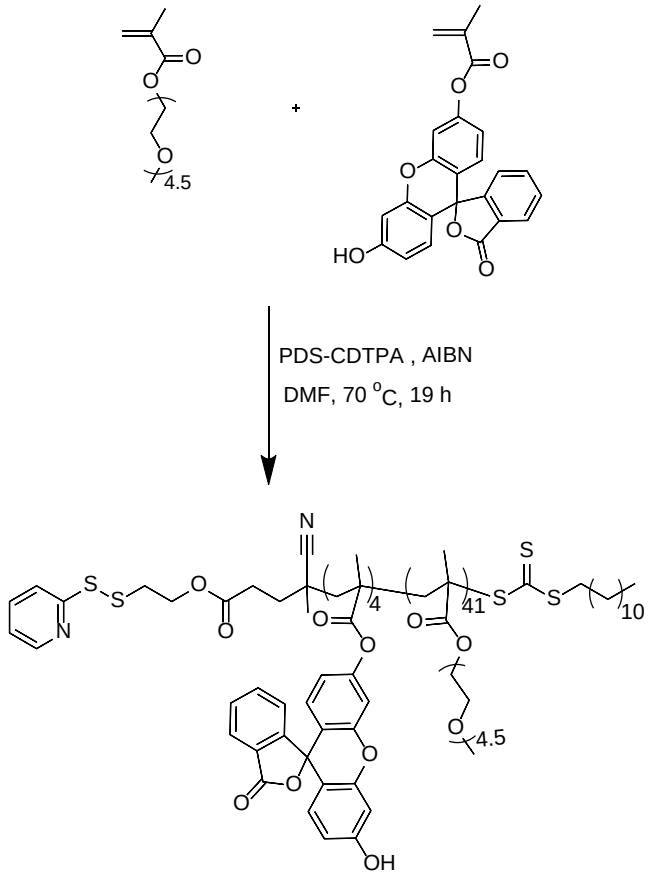

Figure 4.7. The synthesis of PDS-POEGMEMA-FMA copolymer.

Molecular weight (Mn) and molecular weight distribution (Mw / Mn) were determined as 14 kDa and 1.21 by GPC measurements. The ^{1}H NMR spectrum of the synthesized polymer was shown in Figure 4.8.

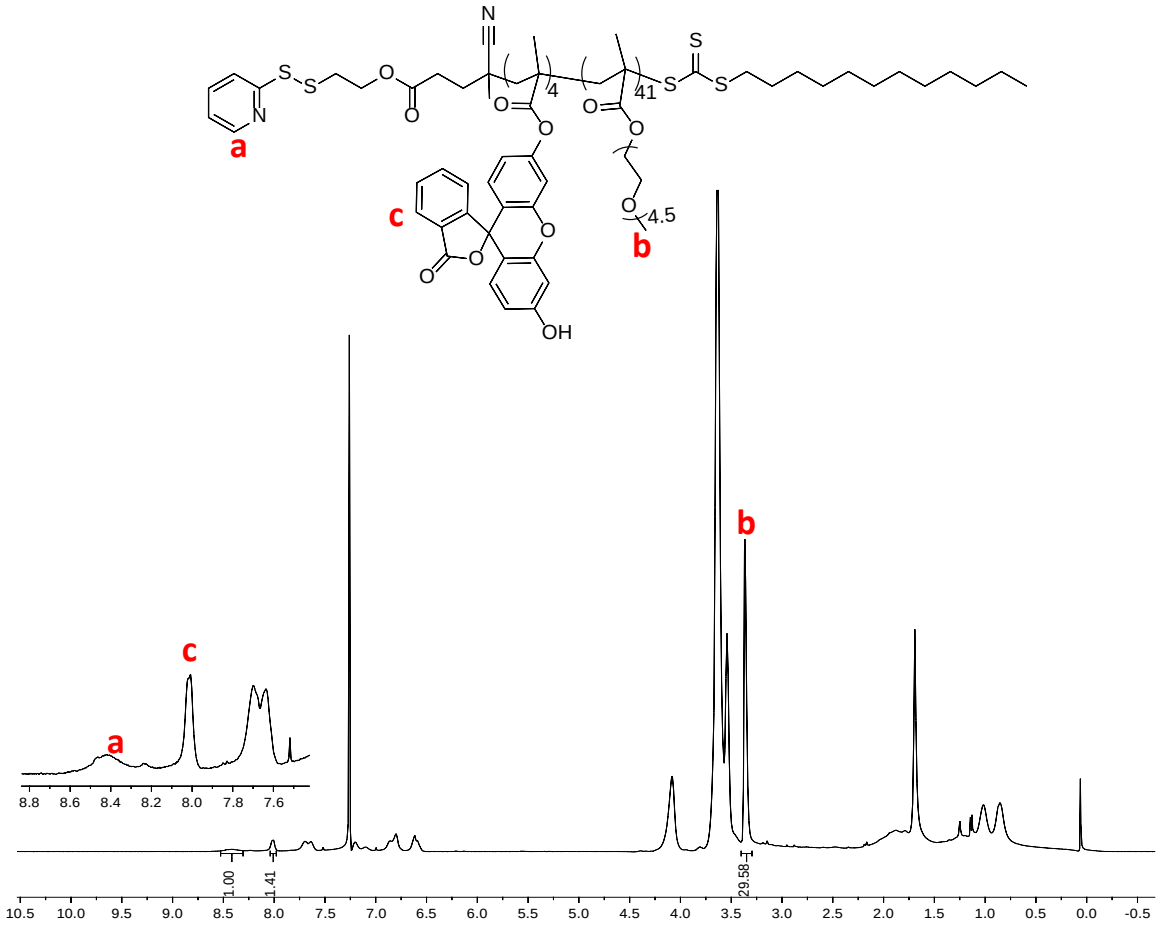

Figure 4.8. ^{1}H NMR spectrum of PDS-POEGMEMA-FMA copolymer.

While, the aromatic proton of pyridine appeared at the peak at 8.42 ppm, the aromatic proton of dye molecule (FMA) appeared at the peak at 8.02 ppm. The peak at 3.37 ppm come from methoxy group of PEGMEMA. The amount of dye was calculated as 12 weight % by ^{1}H NMR spectroscopy. Calibration with FMA was plotted by using Fluorescence Spectroscopy (Figure 4.9).

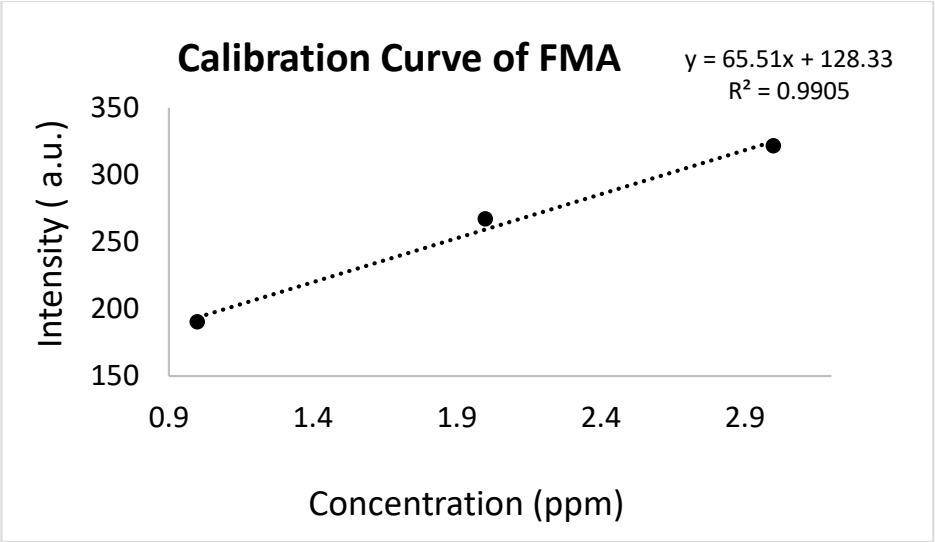

Figure 4.9. The calibration curve of FMA.

4.5. Synthesis of PDS-POEGMEMA-DTX-FMA Copolymer

The dye and drug-containing PDS-POEGMEMA-DTX-FMA copolymer was synthesized by using OEGMEMA, MA-GFLG-DTX, FMA, AIBN and PDS-CDTPA *via* the RAFT polymerization technique (Figure 4.10). Molecular weight (Mn) and molecular weight distribution (Mw / Mn) values were determined as 10 kDa and 1.20 by GPC.

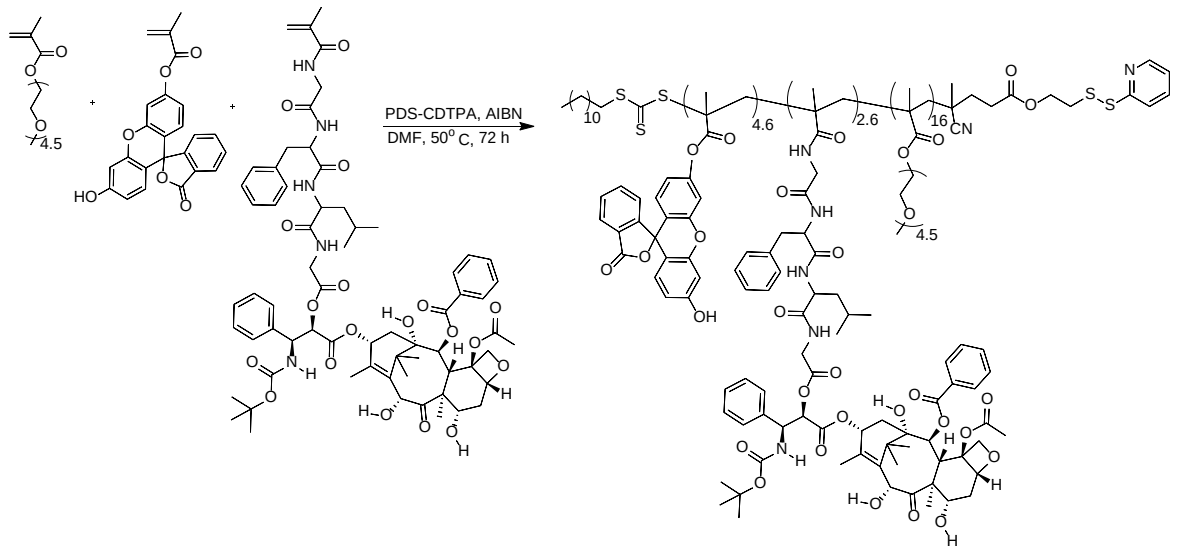

Figure 4.10. Schematic representation of PDS-POEGMEMA-DTX-FMA copolymer.

In the PDS-POEGMEMA-DTX-FMA copolymer, the DTX amount was 5 as weight %. Since the amount of DTX was lower than targeted 10 as weight %, polymers with different amounts of DTX and molecular weight were synthesized by using different ratios of OEGMEMA, MA-GFLG-DTX and FMA monomers. These conditions were shown in Table 4.2.

Table 4.2. Reaction conditions and results for the synthesis of PDS-POEGMEMA-DTX-FMA polymer.

No	**Polymer**	**Equivalents**					**DMF (mL)**	**GPC M_n (kDa)**	**M_w/M_n**	**DTX in Polymer as weight %**
		OEGMEMA	**MA-GFLG-DTX**	**FMA**	**PDS-CDTPA**	**AIBN**				
1	PS1	140	15	25	5	1	1	10	1.20	5
2	PS2	100	14	19	5	1	1.4	10	1.19	20
3	PS3	175	35	20	5	1	2	12	1.20	8.6
4	PS4	100	14	9	5	1	0.9	10	1.21	17
5	PS5	215	25	10	5	1	0.7	20	1.40	8
6	PS6	215	25	10	5	1	0.7	16	1.40	5

^{1}H NMR spectroscopy analysis of PS2 polymer was shown in Figure 4.11. According to ^{1}H NMR spectroscopy result, the peak at 8.09 ppm come from the aromatic proton of DTX and the peak at 7.98 pm belonged to FMA molecule. The amount of DTX in each polymer chain was calculated as 20 weight % by comparing these peaks with each other.

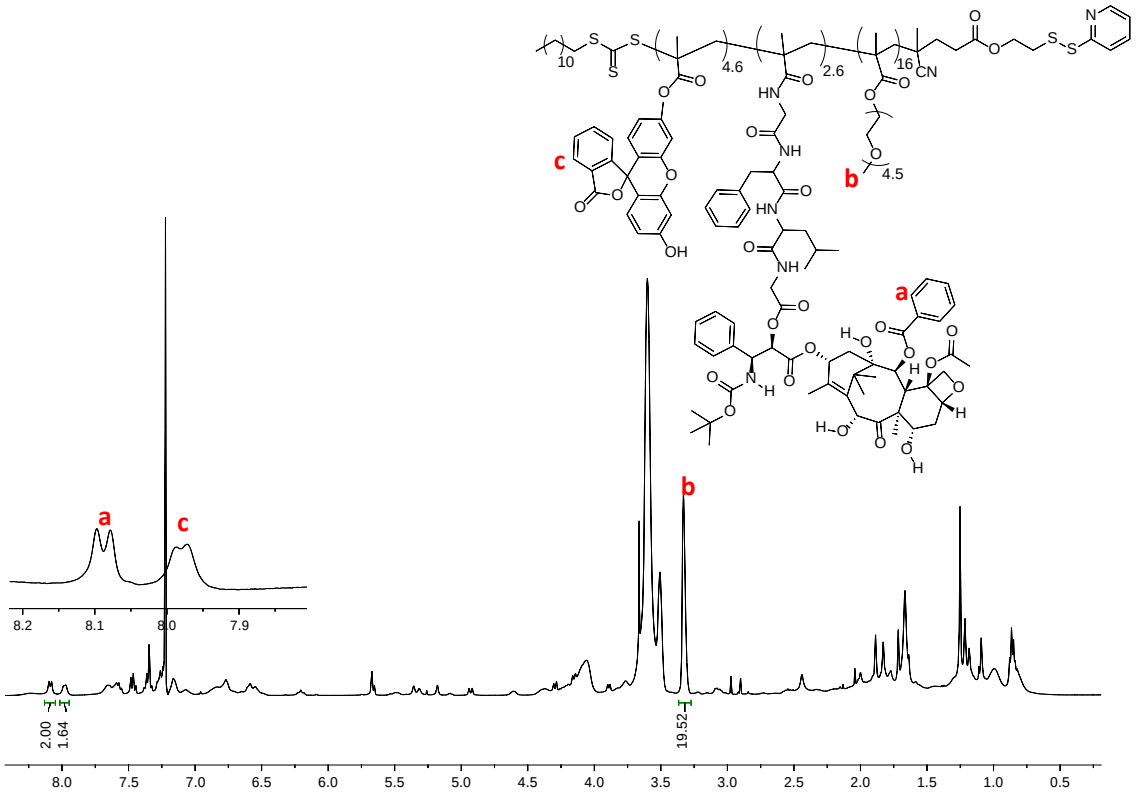

Figure 4.11. ^{1}H NMR spectrum of PDS-POEGMEMA-DTX-FMA copolymer (PS2).

It has been observed that the PS2 polymer has high DTX amount as weight percent, but it has low solubility in water. When 1 mg of polymer was added to 1 mL of water, a cloudy mixture was obtained and precipitation of polymer in water was observed after one day. Solubility is a problem in the conjugation step. Therefore, in order to solve the problem of resolution and drug amount of polymers, new polymers were synthesized by increasing the ratio of OEGMEMA monomer (Table 4.2).

4.6. Synthesis of PDS-POEGMEMA-DTX Copolymer

The drug-containing PDS-POEGMEMA-DTX copolymer was synthesized by using OEGMEMA, MA-GFLG-DTX, AIBN and PDS-CDTPA via the RAFT polymerization technique (Figure 4.12). Molecular weight (Mn) was determined as 19 kDa by GPC. In the PDS-POEGMEMA-DTX copolymer, the drug amount was calculated as 10.6 (weight %) by ^{1}H NMR spectroscopy.

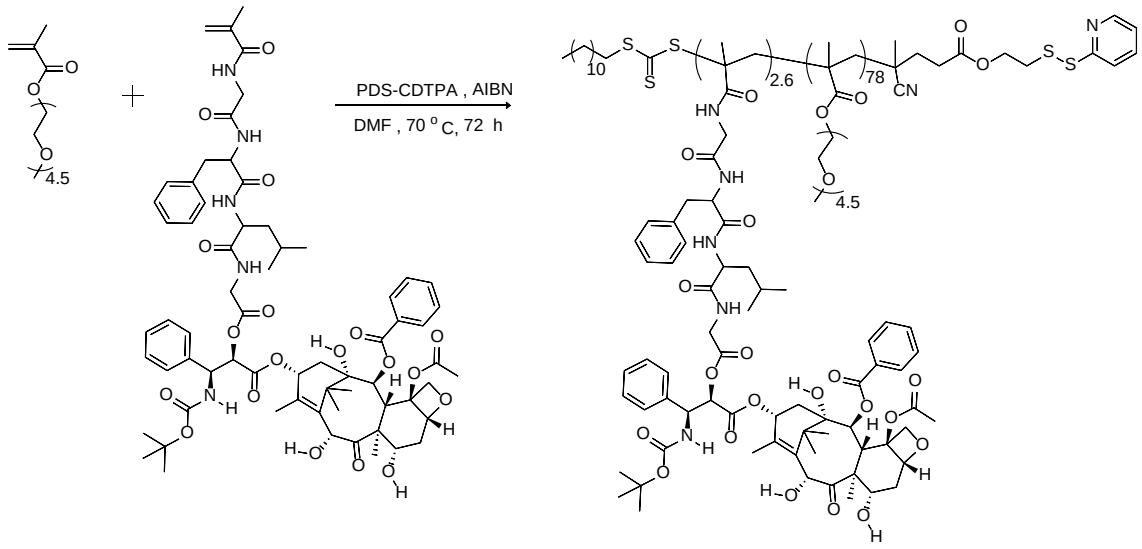

Figure 4.12. Schematic representation of PDS-POEGMEMA-DTX copolymer.

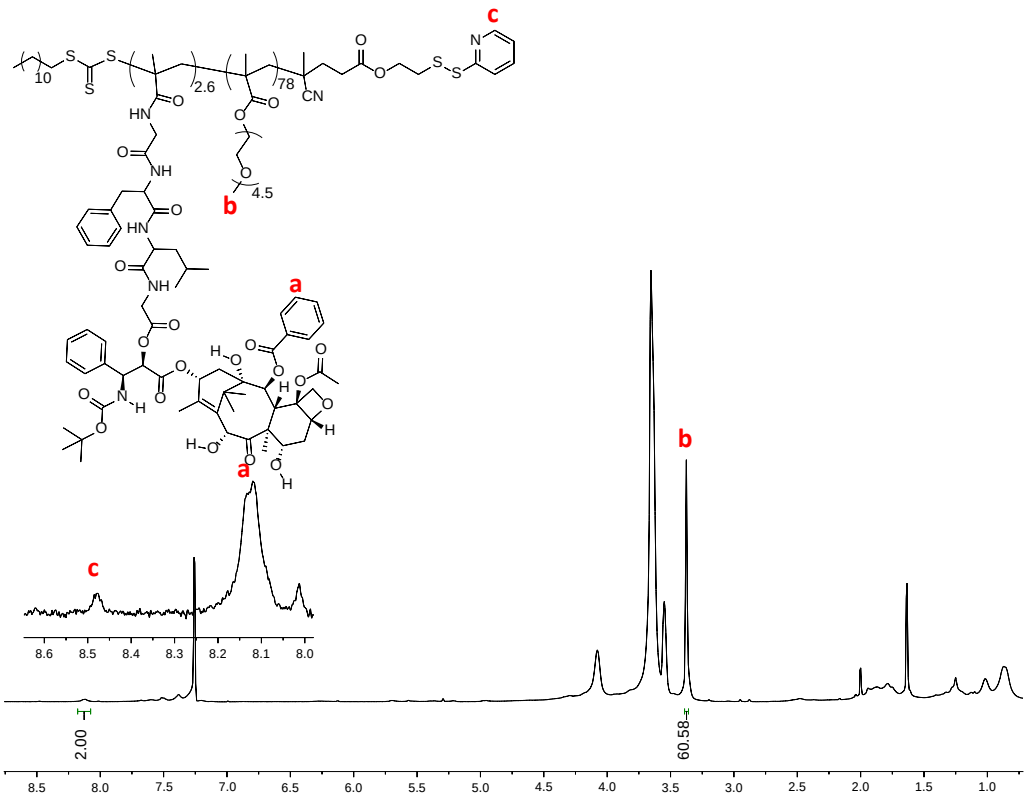

Figure 4.13. ^{1}H NMR characterization of PDS-POEGMEMA-MA-GFLF-DTX copolymer.

According to ^{1}H NMR spectroscopy result, the peak 8.42 ppm represented to an aromatic proton of pyridine and the peak at 8.13 ppm belonged to DTX molecule. The broad singlet at 3.38 ppm come from methoxy group of PEGMEMA.

4.7. Tmab-PDS-POEGMEMA-FMA Conjugation

In order to obtain Tmab-polymer conjugation, amine groups on Tmab were converted to thiol groups by using Traut reagent (Figure 4.14). This process was repeated with 2 different equivalents (25 and 50 times Traut reagent) in order to contain the different number of thiol groups in the reacted Tmab and the equivalent of Traut reagent was determined as 25. At the end of the reaction, sample and Ellman reagent were added to PBS according to Ellman analysis protocol and this solution was measured by UV spectroscopy in order to determine the number of thiol. The number of thiol groups on Tmab was calculated by using the absorbance value at 412 nm. After calculation, the number of thiols on Tmab averagely was obtained as 5.

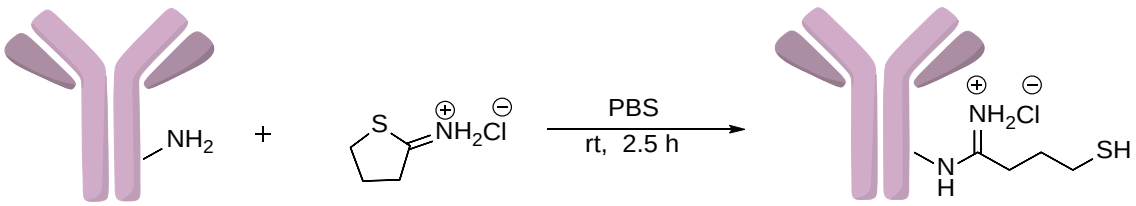

Figure 4.14. Schematic representation of modification of trastuzumab with thiol groups.

Conjugation of the thiolated Tmab with the PDS-POEGMEMA-FMA copolymer was carried out in PBS buffer solution (Figure 4.15). Conjugation trials were started with PDS-POEGMEMA-FMA copolymer in order to determine the condition, time, purification and characterization method for next conjugation with DTX containing copolymers.

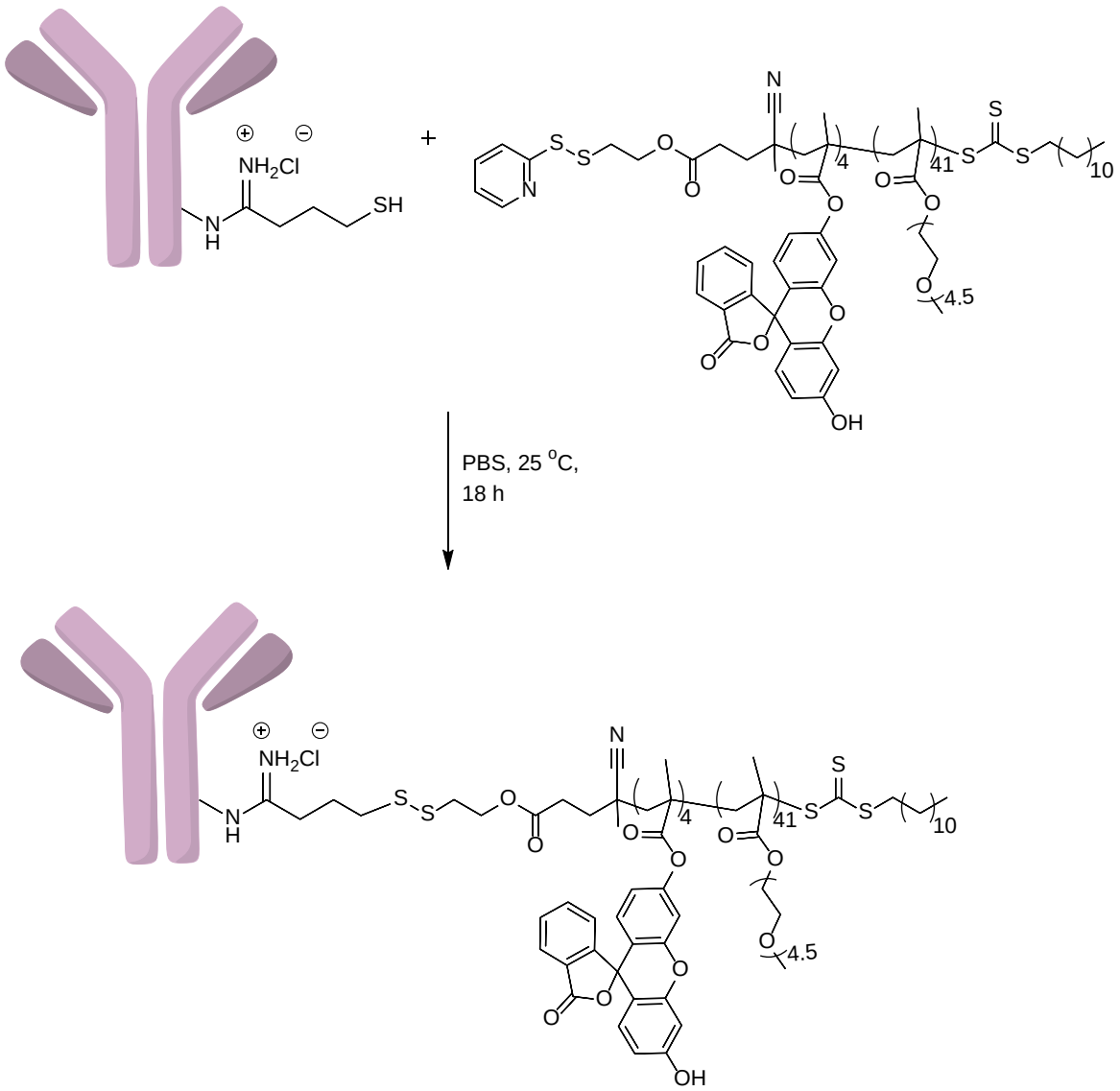

Figure 4.15. Schematic representation of Tmab-PDS-POEGMEMA-FMA conjugation.

The resulting yellow product was dialyzed by using ultra centrifuge filter (30 kDa) to remove unreacted polymers. After dialysis, this yellow product was a visual data to indicate that the dye containing polymer was conjugated to Tmab because yellow color only came from Fluorescein dye.

Fluorescence spectroscopy was used to determine how many polymers were conjugated to Tmab. For this purpose, FMA was dissolved in 0.1 N NaOH because this dye was soluble in basic solution. FMA samples with different concentration were prepared and

a calibration curve was drawn with these solutions via fluorescence spectroscopy (Figure 4.16).

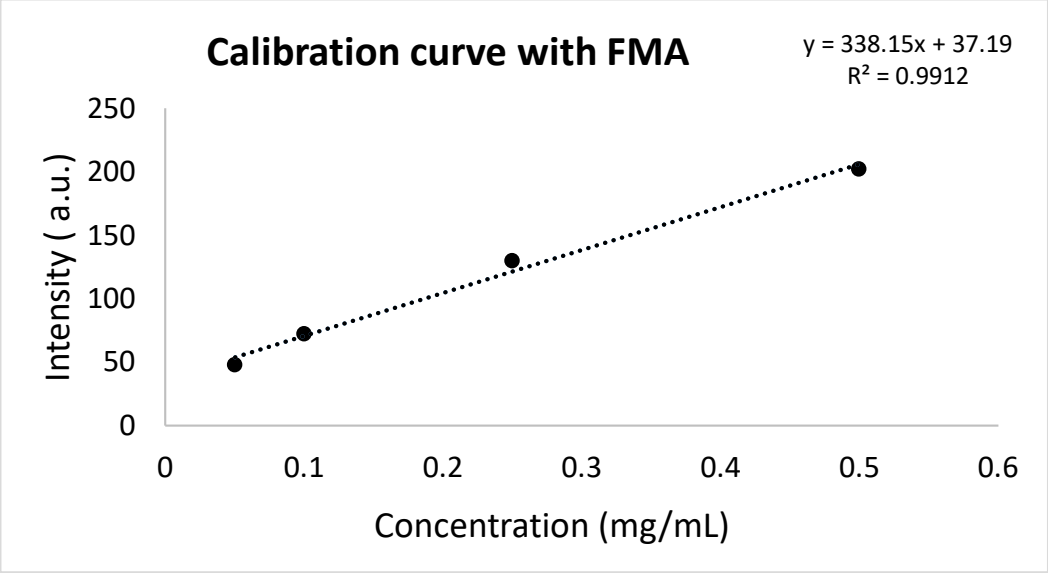

Figure 4.16. The graph of calibration curve with FMA.

The amount of FMA in the polymer used for the conjugation and the amount of FMA contained in the resulting conjugates were calculated by using this calibration curve. As a result of the calculations, FMA / Polymer and FMA / Tmab ratios were determined in terms of concentration. PAR (polymer per antibody ratio) was determined by the calculation shown below.

$$\mathrm{PAR} = \frac{\mathrm{FMA/Tmab}}{\mathrm{FMA/Polymer}}$$

The trial conditions and results of 3 different conjugates synthesized by using PDS-POEGMEMA-FMA copolymer were shown in Table 4.3. In these experiments, it was aimed to observe the effect of polymer / Tmab ratio and reaction concentration on the number of PAR.

Table 4.3. Methods and results of conjugation with Tz-PDS-POEGMEMA-FMA.

No	Conjugate	Tmab	# SH	Polymer	DMAc (µL)	PBS (pH 6.5) (mL)	PAR
1	C1	1	12	8	6	0.128	3.5
2	C2	1	12	8	6	1	2.5
3	C3	1	6	16	6	0.128	2.0

When C1 and C2 were compared, the effect of polymer concentration on PAR was examined. When the concentration increased (C1), PAR also increased, in other words, more polymers were conjugated to a Tmab. When C1 and C3 were compared, the effect of thiol content and polymer / Tmab ratio on PAR was examined. When the amount of thiol groups was reduced by using the same concentration and the amount of polymer was increased, the PAR ratio was 2.

The PDS-POEGMEMA-FMA polymer used in this conjugation contained 4 dyes. The PAR value of the C3 conjugate was 2 and this represented that each Tmab carried 8 dyes. When this amount of dye was considered as drug, DAR (Drug to antibody ratio) value can be supposed as 8. Considering this fact, the DAR value used in the market was approximately 3.5, so the PAR value of obtained conjugate was 2 and it was a promising value.

Although the PAR value was 3.5 in the C1 conjugate, the method in the C3 conjugate was chosen for further experiments. This is due to the fact that if there are more thiols in the C1 conjugate, the increased amount of thiol can change or decrease the activity of the Tmab. If the part of the Tmab to bind to the HER2 receptor is also thiolated and one conjugation from this part is also present, the binding of Tmab to the HER2 receptor may be prevented. This means that the active targeting feature of the conjugate is lost or decreased. When the antibody-drug conjugates used in the market were examined, it was found that when they tried to bound more drugs to the antibody, the activity of the antibody decreased as the DAR increased. Therefore, the main purpose of this thesis is to increase the DAR by increasing

the amount of drug contained in the polymer and by keeping PAR low without affecting the activity of the antibody.

4.8. Purification and Characterization of Tmab-Polymer Conjugates

Purification was carried out for two free products. Firstly, ultra centifuge filter was used to remove free polymer. UV or fluorescence spectroscopy were performed to verify that free polymer was removed from conjugates and free Tmab. Secondly, purification was carried out by using AKTA AVANT instrument via the hydrophobic interaction chromatography column (HIC) to remove free Tmab. The hydrophobic filler material of the HIC column interacts differently with proteins having various surface hydrophobicity. The working mechanism of HIC is based on the differences in the surface hydrophobicity of proteins. Therefore, it is possible to differentiate the proteins in different hydrophobicity with this method. To create these different proteins, proteins are loaded with buffer solutions containing a high amount of salt, and proteins are attached to the column, then proteins are removed from the column with buffer solutions containing low amounts of salt. In the removal step from column, the first protein collected is the one with the less hydrophobic surface, and the protein collected at the latest is the one with the higher hydrophobicity.

Our goal was to find that a method allows free Tmab and conjugates to be connected to the column and then allows them to separate from the column in a specific order. Firstly, free mab was tried with this method, and free mab didn't bind to column and was collected in the column wash step, and its moleculer weight (Mn) was analyzied by SEC-MALLS as 144.7 kDa (Figure 4.17).

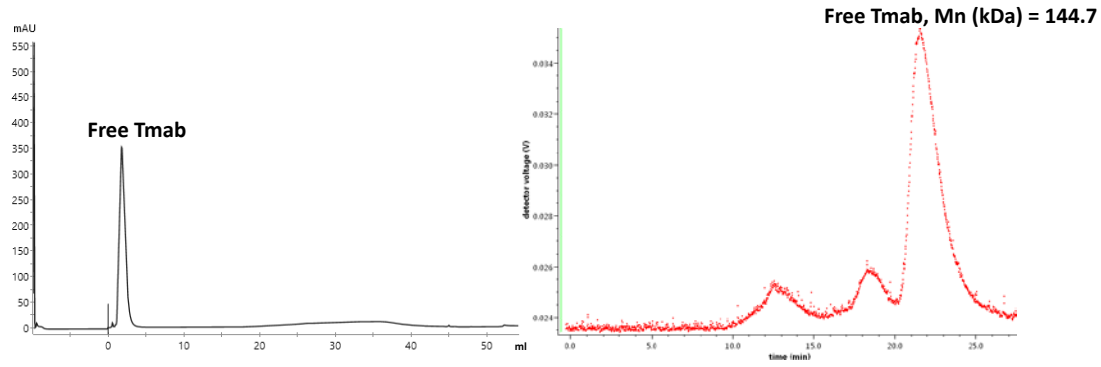

Figure 4.17. The purification result of free mab and its SEC-MALLS's result.

After free mab, the method was used for conjugate reactions and free Tmabs was removed from the column in the column wash step, only the conjugates were attached to the column and removed from the column with pure water in the elution step (Figure 4.18).

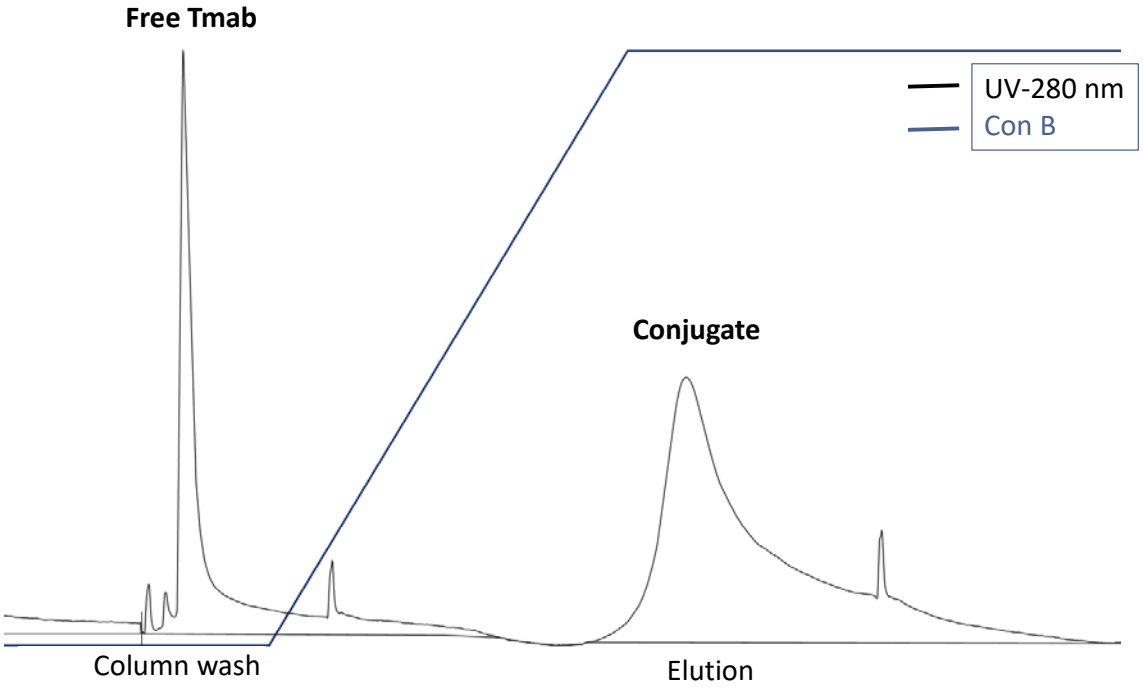

Figure 4.18. Purification via column chromatography of C3.

The number of polymer bound in the purified conjugates was determined by the equation obtained from the calibration curve drawn by the FMA after purification. BCA analysis was performed to determine the amount of protein in the conjugates.

5. CONCLUSION

In this thesis, antibody polymer drug conjugates were synthesized by using copolymers that contained different amounts of PEG, FMA and DTX and thiolated Tmab in the presence of PBS. For this purpose, PDS-POEGMEMA-FMA and PDS-POEGMEMA-DTX-FMA copolymers with different weight percent of FMA and DTX were synthesized by using RAFT polymerization method. In general, PDS-POEGMEMA-DTX-FMA copolymers had DTX 5 - 20 % by weight. Initially, conjugation was accomplished between PDS-POEGMEMA-FMA copolymer and thiolated Tmab and this conjugation was used to optimize reaction condition and purification method. After the reactions, the results showed that two polymers were bound to one molecule of Tmab (PAR = 2). This optimized reaction conditions will be further used to conjugate PDS-POEGMEMA-DTX-FMA copolymer to the thiolated Tmab.

REFERENCES

1. Tsuchikama, K. and Z. An, "Antibody-Drug Conjugates: Recent Advances In Conjugation And Linker Chemistries", *Protein & Cell*, Vol. 9, No.1, pp. 33–46, 2018.

2. Siegel, R., D. Naishadham, and A. Jemal, "Cancer Statistics, 2013", *CA: A Cancer Journal for Clinicians*, Vol. 63, No.1, pp. 11–30, 2013.

3. Bray, F., J. Ferlay, I. Soerjomataram, R.L. Siegel, L.A. Torre, and A. Jemal, "Global Cancer Statistics 2018: Globocan Estimates Of Incidence And Mortality Worldwide For 36 Cancers In 185 Countries", *CA: A Cancer Journal for Clinicians*, Vol. 68, No.6, pp. 394–424, 2018.

4. Nahta, R., D. Yu, M.-C. Hung, G.N. Hortobagyi, and F.J. Esteva, "Mechanisms Of Disease: Understanding Resistance To HER2-Targeted Therapy In Human Breast Cancer", *Nature Clinical Practice Oncology*, Vol. 3, No 1, pp. 269–280, 2006.

5. Bonita, R., and R. Pradhan, "Cardiovascular Toxicities Of Cancer Chemotherapy", *Seminars in Oncology*, Vol. 40, No.2, pp. 156–167, 2013.

6. Friberg, L.E., and M.O. Karlsson, "Mechanistic Models For Myelosuppression", *Investigational New Drugs*, Vol. 21, No.2, pp. 183–194, 2003.

7. Yamashita, F., and M. Hashida, "Pharmacokinetic Considerations for Targeted Drug Delivery", *Advanced Drug Delivery Reviews*, Vol. 65, No.1, pp. 139-147, 2012.

8. Maeda, H., K. Greish, and J. Fang, "The EPR Effect And Polymeric Drugs: A Paradigm Shift For Cancer Chemotherapy In The 21st Century", *Polymer Therapeutics II. Advances in Polymer Science*, Vol. 193, No.1, pp. 103–121, 2005.

9. Marcucci, F. and F. Lefoulon, "Active Targeting With Particulate Drug Carriers In Tumor Therapy: Fundamentals And Recent Progress", *Drug Discovery Today*, Vol. 9, No.5, pp. 219–228, 2004.

10. Sim, E.H., I.A. Yang, R. Wood-Baker, R. V Bowman, and K.M. Fong, “Gefitinib For Advanced Non-Small Cell Lung Cancer”, *Cochrane Database of Systematic Reviews*, Vol. 1, pp. CD006847, 2018.

11. Steino, A., G. He, J.A. Bacha, D.M. Brown, and Z. Siddik, “Abstract 1429: DNA Damage Response To Dianhydrogalactitol (VAL-083) In P53-Deficient Non-Small Cell Lung Cancer Cells”, *Molecular and Cellular Biology, Genetics*, Vol. 77, No.13, pp. 1429–1429, 2017.

12. Nami, B., H. Maadi, and Z. Wang, “Mechanisms Underlying The Action And Synergism Of Trastuzumab And Pertuzumab In Targeting HER2-Positive Breast Cancer”, *Cancers*, Vol. 10, No.10, pp. 342, 2018.

13. Bhatt, S., B.M. Ashlock, Y. Natkunam, V. Sujoy, J.R. Chapman, J.C. Ramos, E.A. Mesri, and I.S. Lossos, “CD30 Targeting With Brentuximab Vedotin: A Novel Therapeutic Approach To Primary Effusion Lymphoma”, *Blood*, Vol. 122, No.7, pp. 1233–42, 2013.

14. DeVita, V.T., and E. Chu, “A History Of Cancer Chemotherapy”, *Cancer Research*, Vol. 68, No. 21, pp. 8643–8653, 2008.

15. Ehrlich, P., “Address In Pathology, On Chemiotherapy: Delivered Before The Seventeenth International Congress Of Medicine”, *British medical journal*, Vol. 2, No. 2746, pp. 353–359, 1913.

16. Mathe, G., L.O.C. Tran Ba, and J. Bernard, “Effect On Mouse Leukemia 1210 Of A Combination By Diazo-Reaction Of Amethopterin And Gamma-Globulins From Hamsters Inoculated With Such Leukemia By Heterografts”, *Comptes rendus hebdomadaires des seances de l’Academie des sciences*, Vol. 246, No. 10, pp. 1626–8, 1958.

17. Sievers, E.L., R.A. Larson, E.A. Stadtmauer *et al*., “Efficacy And Safety Of Gemtuzumab Ozogamicin In Patients With CD33-Positive Acute Myeloid Leukemia In First Relapse”, *Journal of Clinical Oncology*, Vol. 19, No. 13, pp. 3244–3254, 2001.

18. Younes, A., N.L. Bartlett, J.P. Leonard, D.A. Kennedy, C.M. Lynch, E.L. Sievers, and A. Forero-Torres, “Brentuximab Vedotin (SGN-35) For Relapsed CD30-Positive

Lymphomas", *New England Journal of Medicine*, Vol. 363, No. 19, pp. 1812–1821, 2010.

19. LoRusso, P.M., D. Weiss, E. Guardino, S. Girish, and M.X. Sliwkowski, "Trastuzumab Emtansine: A Unique Antibody-Drug Conjugate In Development For Human Epidermal Growth Factor Receptor 2-Positive Cancer", *Clinical Cancer Research*, Vol. 17, No. 20, pp. 6437–6447, 2011.

20. Rudnick, S.I., J. Lou, C.C. Shaller, Y. Tang, A.J.P. Klein-Szanto, L.M. Weiner, J.D. Marks, and G.P. Adams, "Influence Of Affinity And Antigen Internalization On The Uptake And Penetration Of Anti-HER2 Antibodies In Solid Tumors", *Cancer Research*, Vol. 71, No.6, pp. 2250–2259, 2011.

21. Polson, A.G., W.Y. Ho, and V. Ramakrishnan, "Investigational Antibody-Drug Conjugates For Hematological Malignancies", *Expert Opinion on Investigational Drugs*, Vol. 20, No. 1, pp. 75–85, 2011.

22. Teicher, B.A. and R.V.J. Chari, "Antibody Conjugate Therapeutics: Challenges And Potential", *Clinical Cancer Research*, Vol. 17, No. 20, pp. 6389–6397, 2011.

23. King, H.D., G.M. Dubowchik, H. Mastalerz, D. Willner, S.J. Hofstead, R.A. Firestone, S.J. Lasch and P.A. Trail, "Monoclonal Antibody Conjugates Of Doxorubicin Prepared With Branched Peptide Linkers: Inhibition Of Aggregation By Methoxytriethyleneglycol Chains", *Journal of medicinal chemistry*, Vol. 45, No. 19, pp. 4336–43, 2002.

24. Finbloom, D.S., D. Abeles, A. Rifai, and P.H. Plotz, "The Specificity Of Uptake Of Model Immune Complexes And Other Protein Aggregates By The Murine Reticuloendothelial System", *Journal of immunology (Baltimore, Md. : 1950)*, Vol. 125, No. 3, pp. 1060–5, 1980.

25. Lyon, R.P., T.D. Bovee, S.O. Doronina, P.J. Burke, J.H. Hunter, H.D. Neff-LaFord, M. Jonas, M.E. Anderson, J.R. Setter and P.D. Senter, "Reducing Hydrophobicity Of Homogeneous Antibody-Drug Conjugates Improves Pharmacokinetics And Therapeutic Index", *Nature Biotechnology*, Vol. 33, No. 7, pp. 733–735, 2015.

26. Zhao, R.Y., S.D. Wilhelm, C. Audette, G. Jones, B.A. Leece, A.C. Lazar, V.S. Goldmacher, R. Singh, Y. Kovtun, W.C. Widdison, J.M. Lambert, and R.V.J. Chari, "Synthesis And Evaluation Of Hydrophilic Linkers For Antibody–Maytansinoid Conjugates", *Journal of Medicinal Chemistry*, Vol. 54, No. 10, pp. 3606–3623, 2011.

27. Kern, J.C., M. Cancilla, D. Dooney, K. Kwasnjuk, R. Zhang, M. Beaumont, I. Figueroa, S. Hsieh, L. Liang, D. Tomazela, J. Zhang, P.E. Brandish, A. Palmieri, P. Stivers, M. Cheng, G. Feng, P. Geda, S. Shah, A. Beck, D. Bresson, J. Firdos, D. Gately, N. Knudsen, A. Manibusan, P.G. Schultz, Y. Sun and R.M. Garbaccio, "Discovery Of Pyrophosphate Diesters As Tunable, Soluble, And Bioorthogonal Linkers For Site-Specific Antibody–Drug Conjugates", *Journal of the American Chemical Society*, Vol. 138, No. 4, pp. 1430–1445, 2016.

28. Chari, R.V.J., "Targeted Cancer Therapy: Conferring Specificity To Cytotoxic Drugs", *Accounts of Chemical Research*, Vol. 41, No. 1, pp. 98–107, 2008.

29. Lazar, A.C., L. Wang, W.A. Blättler, G. Amphlett, J.M. Lambert and W. Zhang, "Analysis Of The Composition Of Immunoconjugates Using Size-Exclusion Chromatography Coupled To Mass Spectrometry", *Rapid Communications in Mass Spectrometry*, Vol. 19, No. 13, pp. 1806–1814, 2005.

30. Junutula, J.R., H. Raab, S. Clark, S. Bhakta, D.D. Leipold, S. Weir, Y. Chen, M. Simpson, S.P. Tsai, M.S. Dennis, Y. Lu, Y.G. Meng, C. Ng, J. Yang, C.C. Lee, E. Duenas, J. Gorrell, V. Katta, A. Kim, K. McDorman, K. Flagella, R. Venook, S. Ross, S.D. Spencer, W. Lee Wong, H.B. Lowman, R. Vandlen, M.X. Sliwkowski, R.H. Scheller, P. Polakis, and W. Mallet, "Site-Specific Conjugation Of A Cytotoxic Drug To An Antibody Improves The Therapeutic Index", *Nature Biotechnology*, Vol. 26, No. 8, pp. 925–932, 2008.

31. Behrens, C.R., E.H. Ha, L.L. Chinn, S. Bowers, G. Probst, M. Fitch-Bruhns, J. Monteon, A. Valdiosera, A. Bermudez, S. Liao-Chan, T. Wong, J. Melnick, J.-W. Theunissen, M.R. Flory, D. Houser, K. Venstrom, Z. Levashova, P. Sauer, T.-S. Migone, E.H. van der Horst, R.L. Halcomb and D.Y. Jackson, "Antibody–Drug Conjugates (ADCs) Derived From Interchain Cysteine Cross-Linking Demonstrate Improved Homogeneity And Other Pharmacological Properties Over Conventional Heterogeneous ADCs",

Molecular Pharmaceutics, Vol. 12, No. 11, pp. 3986–3998, 2015.

32. Bryden, F., A. Maruani, H. Savoie, V. Chudasama, M.E.B. Smith, S. Caddick and R.W. Boyle, "Regioselective And Stoichiometrically Controlled Conjugation Of Photodynamic Sensitizers To A HER2 Targeting Antibody Fragment", *Bioconjugate Chemistry*, Vol. 25, No. 3, pp. 611–617, 2014.

33. Tolcher, A.W., S. Sugarman, K.A. Gelmon, R. Cohen, M. Saleh, C. Isaacs, L. Young, D. Healey, N. Onetto and W. Slichenmyer, "Randomized Phase II Study Of BR96-Doxorubicin Conjugate In Patients With Metastatic Breast Cancer", *Journal of Clinical Oncology*, Vol. 17, No. 2, pp. 478–478, 1999.

34. Laguzza, B.C., C.L. Nichols, S.L. Briggs, G.J. Cullinan, D.A. Johnson, J.J. Starling, A.L. Baker, T.F. Bumol and J.R. Corvalan, "New Antitumor Monoclonal Antibody-Vinca Conjugates LY203725 And Related Compounds: Design, Preparation, And Representative In Vivo Activity", *Journal of medicinal chemistry*, Vol. 32, No. 3, pp. 548–55, 1989.

35. Gondi, C.S. and J.S. Rao, "Cathepsin B As A Cancer Target", *Expert Opinion on Therapeutic Targets*, Vol. 17, No. 3, pp. 281–291, 2013.

36. Dubowchik, G.M., R.A. Firestone, L. Padilla, D. Willner, S.J. Hofstead, K. Mosure, J.O. Knipe, S.J. Lasch and P.A. Trail, "Cathepsin B-Labile Dipeptide Linkers For Lysosomal Release Of Doxorubicin From Internalizing Immunoconjugates: Model Studies Of Enzymatic Drug Release And Antigen-Specific In Vitro Anticancer Activity", *Bioconjugate chemistry*, Vol. 13, No. 4 pp. 855–69, 2002.

37. Hartley, J.A., "The Development Of Pyrrolobenzodiazepines As Antitumour Agents", *Expert Opinion on Investigational Drugs*, Vol. 20, No. 6, pp. 733–744, 2011.

38. Wu, G., Y.-Z. Fang, S. Yang, J.R. Lupton and N.D. Turner, "Glutathione Metabolism And Its Implications For Health", *The Journal of Nutrition*, Vol. 134, No. 3, pp. 489–492, 2004.

39. Mills, B.J., and C.A. Lang, "Differential Distribution Of Free And Bound Glutathione And Cyst(E)Ine In Human Blood", *Biochemical Pharmacology*, Vol. 52, No. 3, pp. 401–

406, 1996.

40. Verma, S., D. Miles, L. Gianni, I.E. Krop, M. Welslau, J. Baselga, M. Pegram, D.-Y. Oh, V. Diéras, E. Guardino, L. Fang, M.W. Lu, S. Olsen, K. Blackwell and EMILIA Study Group, "Trastuzumab Emtansine For HER2-Positive Advanced Breast Cancer", *New England Journal of Medicine*, Vol. 367, No. 19, pp. 1783–1791, 2012.

41. Nuti, M., F. Bellati, V. Visconti, C. Napoletano, L. Domenici, J. Caccetta, I.G. Zizzari, I. Ruscito, H. Rahimi, P. Benedetti-Panici, and A. Rughetti, "Immune Effects Of Trastuzumab", *Journal of Cancer*, Vol. 2, pp. 317–23, 2011.

42. Tian, X., J. Ding, B. Zhang, F. Qiu, X. Zhuang, Y. Chen, X. Tian, J. Ding, B. Zhang, F. Qiu, X. Zhuang and Y. Chen, "Recent Advances In RAFT Polymerization: Novel Initiation Mechanisms And Optoelectronic Applications", *Polymers*, Vol. 10, No. 3, pp. 318, 2018.

43. Moad, G., E. Rizzardo and S.H. Thang, "Radical Addition–Fragmentation Chemistry In Polymer Synthesis", *Polymer*, Vol. 49, No. 5, pp. 1079–1131, 2008.

44. Derek L. Patton, Matthew Mullings and Timothy Fulghum, and R.C. Advincula, "A Facile Synthesis Route To Thiol-Functionalized α,ω-Telechelic Polymers Via Reversible Addition Fragmentation Chain Transfer Polymerization", *Macromolecules,* Vol. 38, No. 20, pp. 8597-8602, 2005.

45. Moad, G., Y.K. Chong, A. Postma, E. Rizzardo and S.H. Thang, "Advances In RAFT Polymerization: The Synthesis Of Polymers With Defined End-Groups", *Polymer*, Vol. 46, No. 19, pp. 8458–8468, 2005.

46. Ulbrich, K., V. Šubr, J. Strohalm, D. Plocová, M. Jelínková and B. Říhová, "Polymeric Drugs Based On Conjugates Of Synthetic And Natural Macromolecules: I. Synthesis And Physico-Chemical Characterisation", *Journal of Controlled Release*, Vol. 64, No. 1-3, pp. 63–79, 2000.

47. Ray, A., N. Larson, D.B. Pike, M. Grüner, S. Naik, H. Bauer, A. Malugin, K. Greish and H. Ghandehari, "Comparison Of Active And Passive Targeting Of Docetaxel For Prostate Cancer Therapy By HPMA Copolymer-RGDfK Conjugates", *Molecular*

pharmaceutics, Vol. 8, No. 4, pp. 1090–1099, 2011.

48. Ruan, Z., P. Yuan, T. Li, Y. Tian, Q. Cheng and L. Yan, "Glutathione Triggered Near Infrared Fluorescence Imaging-Guided Chemotherapy By Cyanine Conjugated Polypeptide", *ACS Biomaterials Science & Engineering*, Vol. 4, No. 12, pp. 4208–4218, 2018.

49. Eyer, P., F. Worek, D. Kiderlen, G. Sinko, A. Stuglin, V. Simeon-Rudolf, and E. Reiner, "Molar Absorption Coefficients For The Reduced Ellman Reagent: Reassessment", *Analytical Biochemistry*, Vol. 312, No. 2, pp. 224–227, 2003.

50. Peterson, G.L., "A Simplification Of The Protein Assay Method Of Lowry Et Al. Which Is More Generally Applicable", *Analytical Biochemistry*, Vol. 83, No. 2, pp. 346–356, 1977.

APPENDIX A: ADDITIONAL DATA

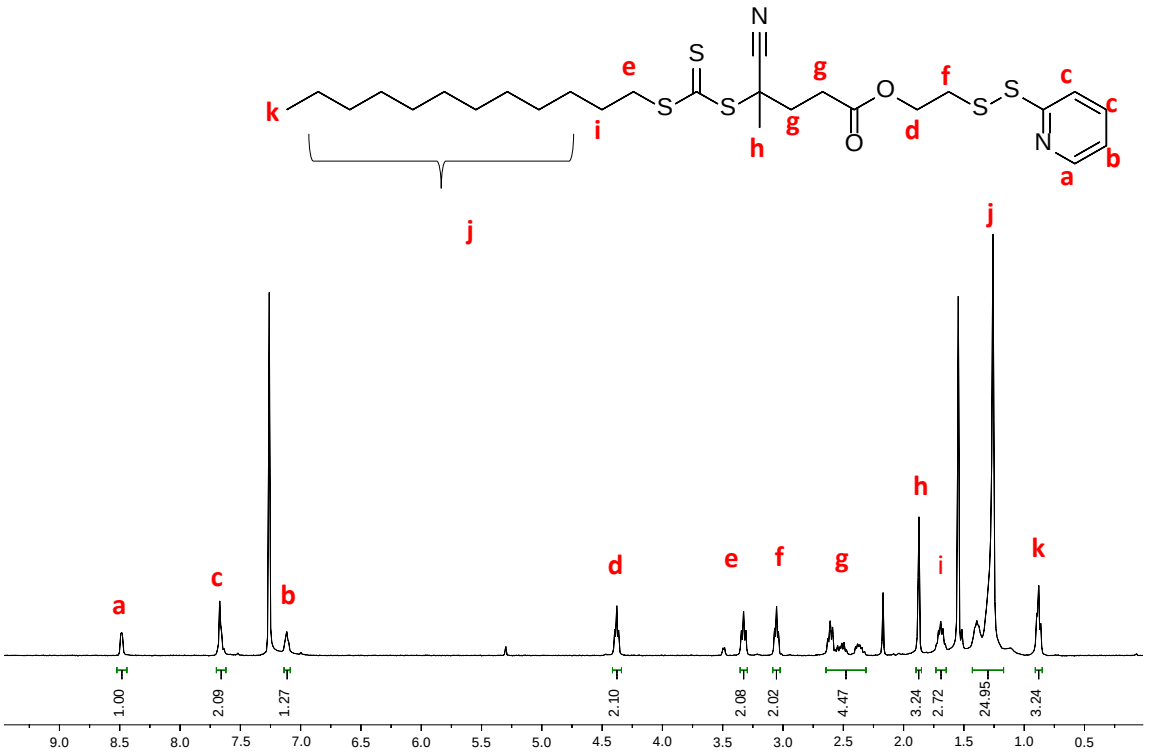

Figure A. 1. ^{1}H NMR spectrum of PDS-CDTPA molecule.

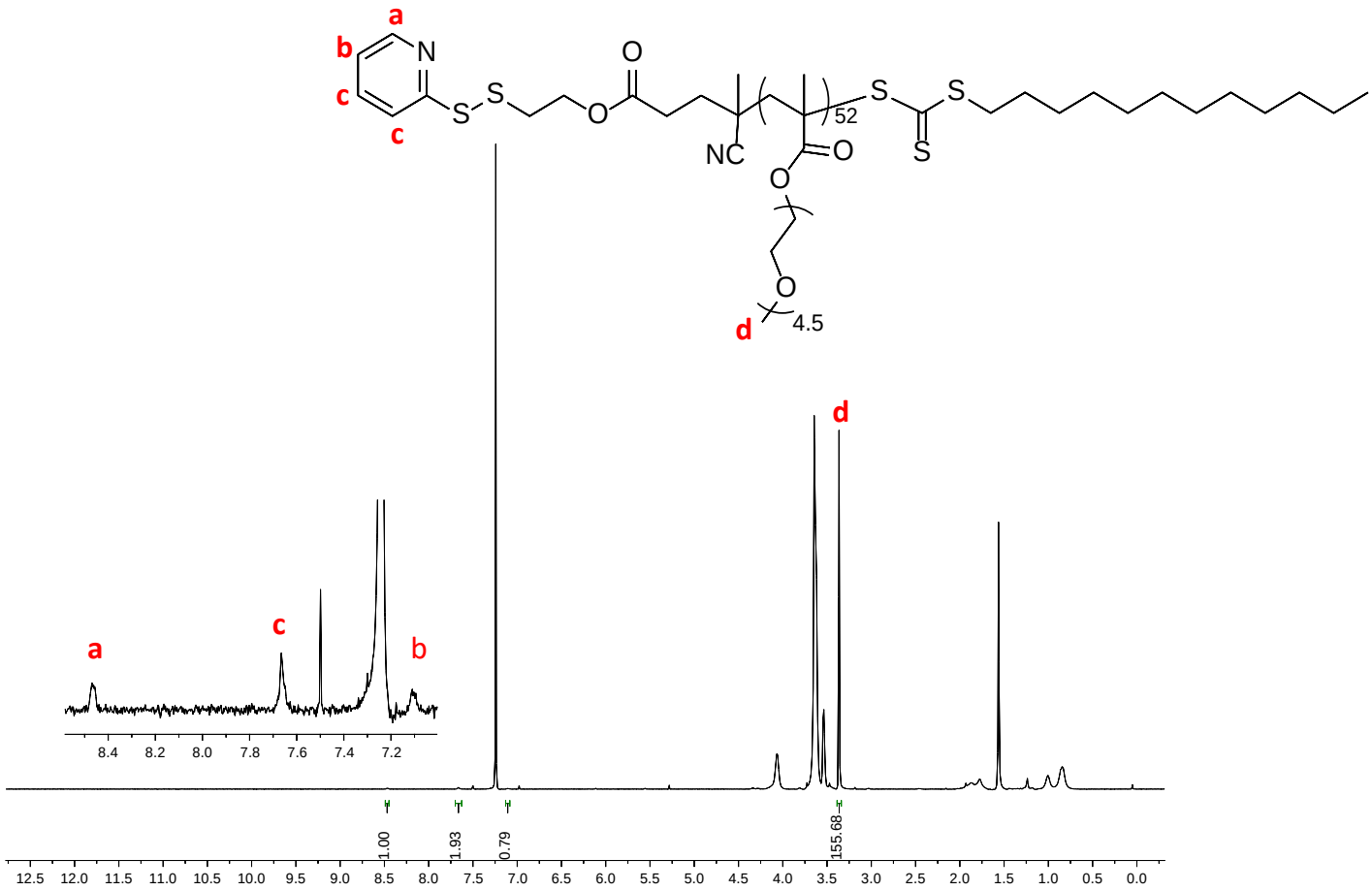

Figure A. 2. ^{1}H NMR spectrum of PDS-POEGMEMA polymer.

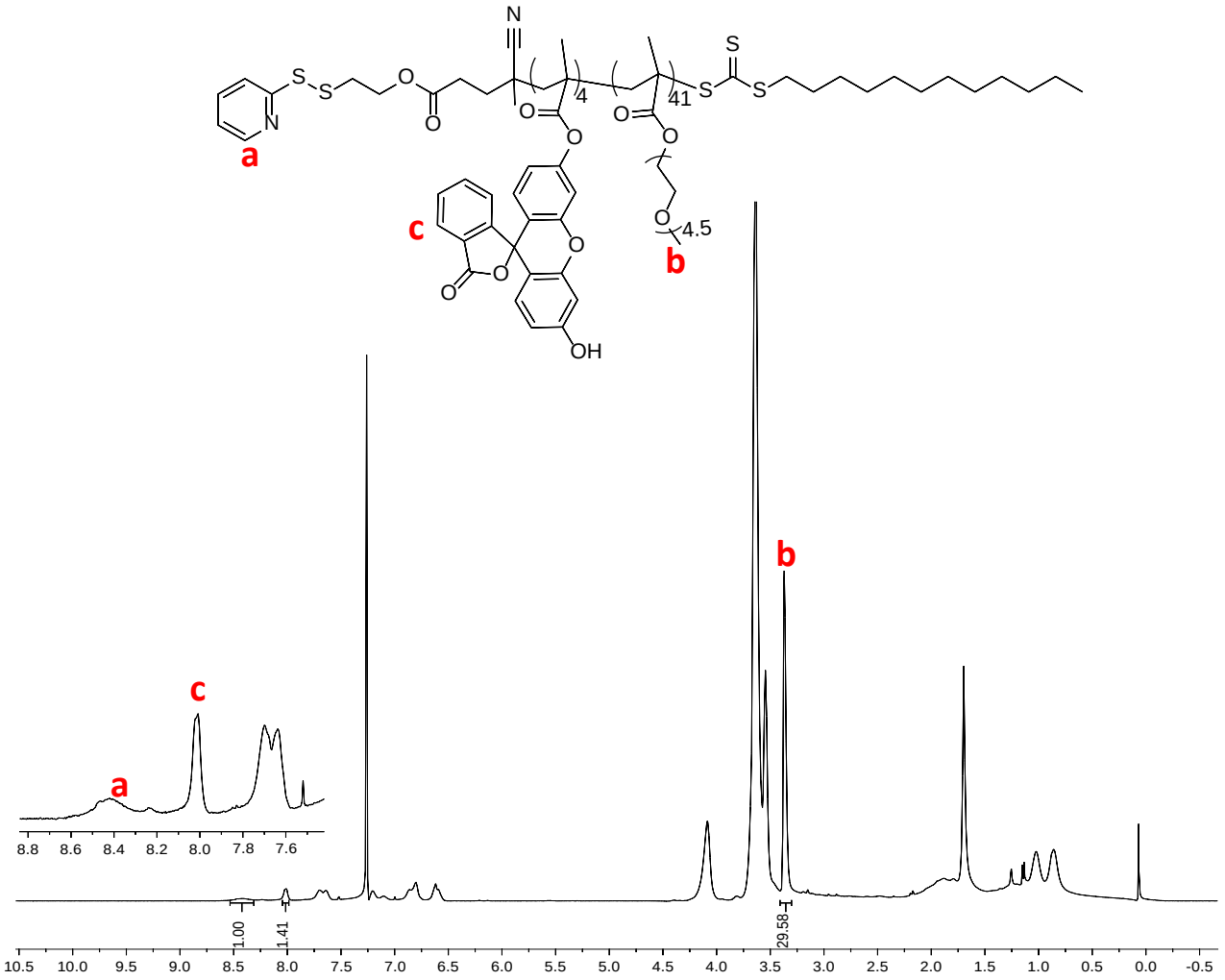

Figure A. 3. ^{1}H NMR spectrum of PDS-POEGMEMA-FMA copolymer.

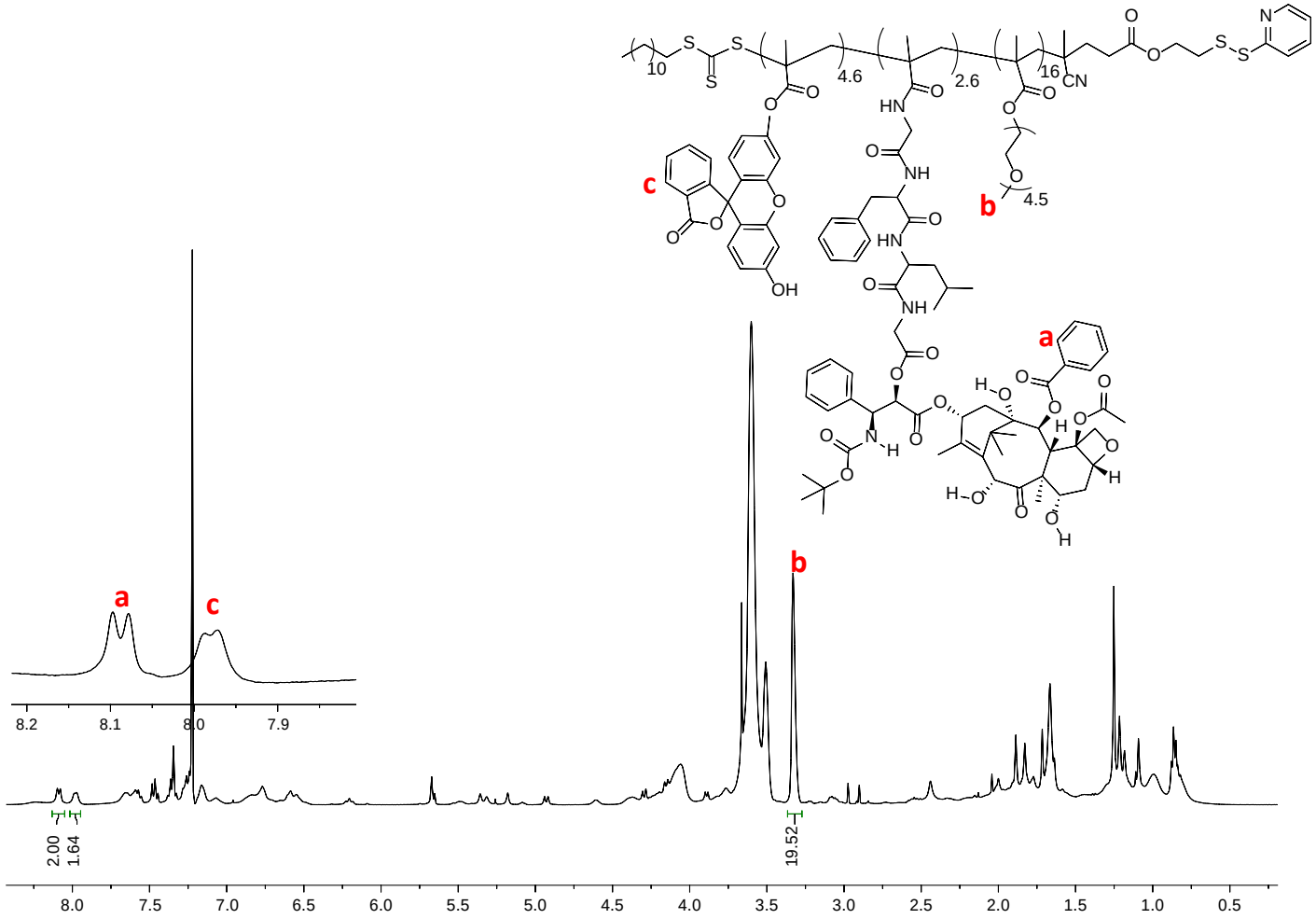

Figure A. 4. ^{1}H NMR spectrum of PDS-POEGMEMA-DTX-FMA copolymer (PS2).

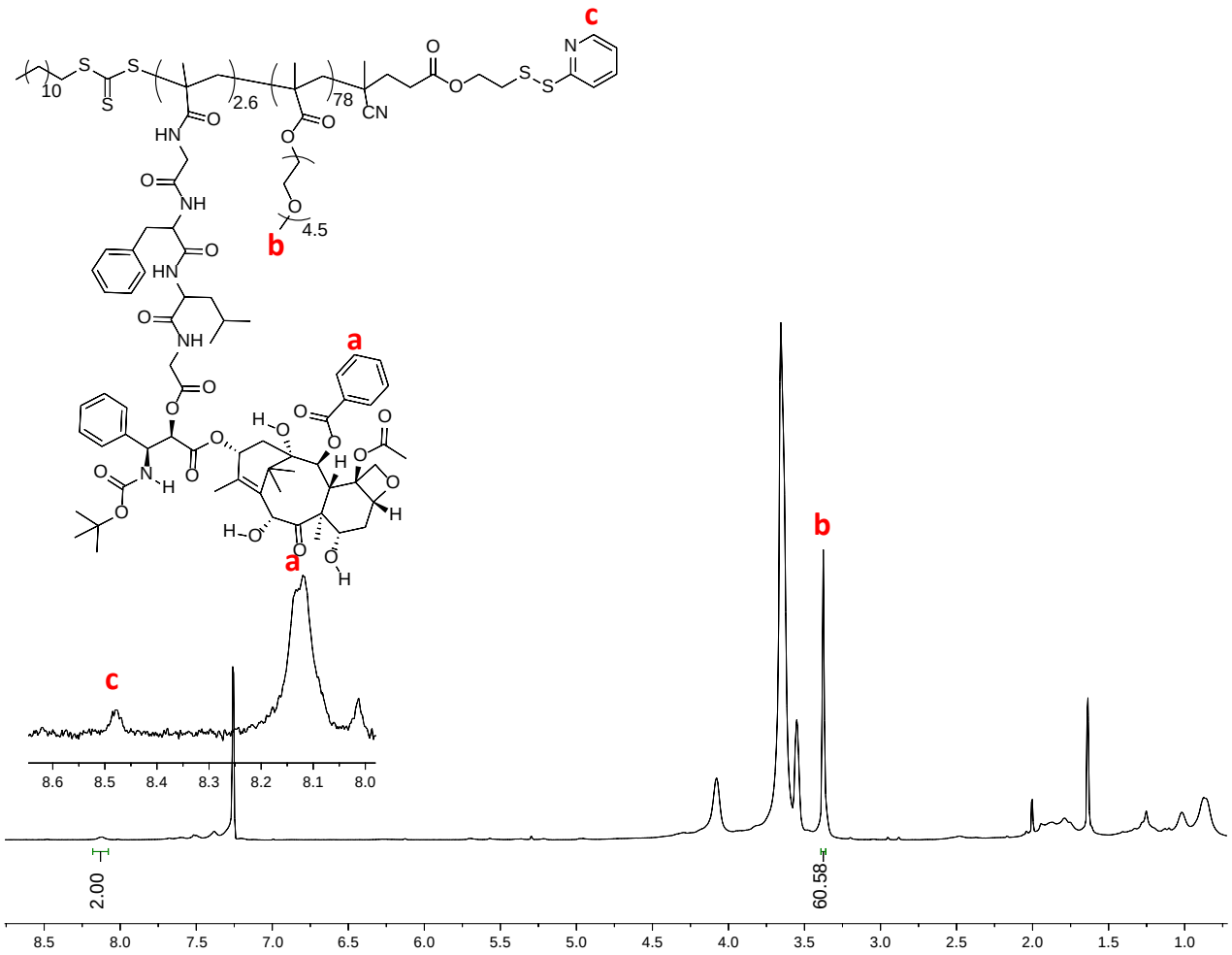

Figure A. 5. ^{1}H NMR characterization of PDS-POEGMEMA-MA-GFLF-DTX copolymer.